INSTITUTO POLITÉCNICO DE BRAGANÇA
Escola Superior de Tecnologia e Gestão

NEW DEVELOPMENTS FOR THE CALCULATION OF THE SAGGING MOMENT RESISTANCE ON COMPOSITE SLABS WITH STEEL DECK EXPOSED TO FIRE

Student:

Abid Tahraoui - a46644

Master Degree In Construction Engineering

Supervised by:

Prof. Paulo Piloto
Prof. Nouredine Benlakehal

Bragança 2021

Dedication

It is with great pleasure that I dedicate this modest work to spirit of my dearest parents, brothers and sisters,

Your love, the values transmitted, your support in the most difficult moments and your constant attention for your children. I boast, every day since the beginning of my life, even without words, of the pride I take in being your child. No matter what happens, making you proud is also one of my goals.

To the whole Construction engineering family,

Our paths crossed for the first time when we entered the IPB , keeping the friendship and international relation that unites us and the memories of all the moments we spent together, nothing to say, I treasure each and every one of the moments we spent with you.

To everyone who has contributed in any way to the smooth running of my work.

Acknowledgements

First and foremost, I would like to thank God for taking me through the most challenging and incredible episode of my life. Furthermore,I would like to dedicate this work to the spirit of my parents, who always dreamed of see me in this place. Also express my deep gratitude to my brothers, sisters and grandmother who have always supported me in the most difficult times. Special thanks to my supervisor at IPB, Prof. Dr Paulo Alexandre Gonçalves Piloto and my supervisor at UHBC: Prof. Dr. Nourredine Benlakehal, for their invaluable support, patience and guidance throughout the development of this work. Thank you for sharing the expertise and providing important advice that made this project possible. Completing this investigation would have been much more difficult without advices, suggestions and support provided by Prof. Dr Abdelkader BOUGARA, Prof. Abderrahmane Habbar and my friends.

Abstract

This work is developed using the 2D finite element method using non-linear thermal analysis. Different slab geometries (re-entrant and trapezoidal) were simulated, using different concrete thicknesses. This composite solution consists of a concrete coating poured onto a steel deck. Concrete is usually reinforced with a steel mesh, but it can also contain individual steel bars. This composite solution is widely used in all types of buildings and the solution method requires the characterization of the materials at elevated temperature in accordance with regulations and standards. The composite slab must meet the fire safety requirements of the building code. The fire resistance of these items is usually evaluated using standard fire resistance tests. Test samples are being prepared in agreement with the materials at elevated temperature and thermal resistance between the steel deck and the concrete must be considered. Annexe D of EN 1994-1-2 provides guidelines for the temperature calculation of the 4 components (every part of steel deck: lower flange, web, and upper flange and rebars) and also calculation the sagging moment of a composite slab with steel deck. However, in the past two decades, no revisions have been made to these methods. The main work developed in this thesis consists of the development of numerical models for thermal analysis, using the ANSYS software. In order to study the effects of different parameters on the sagging moment of the composite slab. A total of 24 numerical simulations were carried out considering an air gap between the steel deck and the concrete topping. The results show that the calculation rules given in European standards are generally conservatives and do not consider important parameters.

Keywords: *Composite slabs with steel deck, Fire resistance, Sagging moment*

RESUMO

Este trabalho foi desenvolvido utilizando o método dos elementos finitos (2D), utilizando análise térmica não linear. Diferentes geometrias de laje (reentrante e trapezoidal) devem ser testadas, utilizando diferentes espessuras de concreto. Esta solução composta consiste em um revestimento de concreto derramado sobre uma plataforma de aço. O beteo é geralmente reforçado com uma malha de aço, mas também pode conter barras de aço individuais. Esta solução composta é amplamente utilizada em todos os tipos de edifícios e o método de solução requer a caracterização dos materiais em temperatura elevada de acordo com os regulamentos e normas. A laje composta deve atender aos requisitos de segurança contra incêndio do regulamento de construção. A resistência ao fogo desses itens é geralmente avaliada por meio de testes padrão de resistência ao fogo. As amostras de teste estão sendo preparadas de acordo com os materiais em temperatura elevada e a resistência térmica entre o deck de aço e o concreto deve ser considerada. O anexo D o EN 1994-1-2 fornece diretrizes para o cálculo da temperatura dos 4 componentes (todas as partes do deck de aço: flange inferior, alma e flange superior e vergalhões) e também o cálculo do momento de flexeo de uma laje mista com deck de aço. No entanto, nas últimas duas décadas, não foram feitas revisões a estes métodos. O principal trabalho desenvolvido nesta tese consiste no desenvolvimento de modelos numéricos para análises térmicas, utilizando o software ANSYS. Para estudar os efeitos de diferentes parâmetos o momento de flexeo da laje mista foram realizadas 24 simulações numéricas considerando um entreferro entre o tabuleiro de aço e a cobertura de concreto. Os resultados mostram que as regras de cálculo indicadas nas normas europeias são geralmente conservadoras e não consideram parâmetros importantes .

Palavras-chave

Lajes compostas com deck de aço, Resistência ao fogo, Momento de flexeo

Contents

List of Tables

List of Figures

Latin letters

A/L_r	The rib geometry factor
A_t	Total area of enclosure (walls, ceiling and floor, including openings)
A_v	Total are of vertical openings on all walls
b	Thermal absorptivity for the total enclosure
c	Specific heat
c_a	Specific heat of carbon steel
c_{air}	Specific heat of air
c_p	Specific heat of dry concrete
$c_{p,peak}$	Peak of specific heat of concrete according to a certain moisture content
D	Maximum deflection
d	Distance from the extreme fibre of the cold design compression zone to the extreme fibre of the cold design tensile zone
d'_{reb}	Concrete cover for rebar
E	Integrity criterion
E_b	Maximum amount of thermal radiation which can be emitted from a surface
h_1	Height of the concrete part of a composite slab above the steel deck
h_2	Height of the concrete part of a composite slab within the steel deck
h_3	Thickness of the screed situated on top of the concrete
h_{eff}	Effective thickness of a composite slab
h_{eq}	Weighted average of window heights on all walls
$\dot{h}_{net}$	Design value of the net heat flux per unit area
$\dot{h}_{cd}$	Conduction heat flux
$\dot{h}_{net,cv}$	Design value of the net heat flux per unit area by convection
$\dot{h}_{net,r}$	Design value of the net heat flux per unit area by radiation
I	Thermal insulation criterion
L	Clear span of the structural element
l_1, l_2, l_3	Specific dimensions of the trapezoidal or re-entrant steel deck profile
n	Normal vector
O	Opening factor of the fire compartment
Q	External heat flux
$q_{t,d}$	Design fire load density related to the total surface area A_t

Q	External heat flux
$q_{t,d}$	Design fire load density related to the total surface area A_t
R	Load bearing criterion
s_{mesh}	Anti-crack mesh spacing
T	The temperature
T_∞	Bulk temperature
$\dot{T}$	Time derivative
T_0	Initial temperature
T_{crit}	Critical temperature of the composite slab
T_g	Gas temperature
t	Time
t_a	Air gap thickness
t_d	Thickness of the steel deck profile
t_{fi}	The fire resistance with respect to thermal insulation criterion
$t_{fi,d}$	Design value of standard fire resistance of a member in fire situation
$t_{fi,r}$	Required standard fire resistance in the fire situation
t_{lim}	Time for maximum gas temperature in case of fuel controlled fire
t_{max}	Time for maximum gas temperature
U	Internal energy
u	Moisture content
u_1; u_2	Shortest distance of the centre of the rebar to any point of the webs of the steel deck
u_3	Distance of the centre of the rebar to the lower flange

Greek letters

α	Angle of the web
α_{cv}	Convective heat transfer coefficient
Δ	Variation
ε	Emissivity
ε_f	Emissivity coefficient of the fire
ε_m	Emissivity coefficient related to the surface material of the member
ε_{res}	Resulting emissivity
Φ	View factor
Φ_{low}	View factor of the lower flange
Φ_{up}	View factor of the upper flange
Φ_{web}	View factor of the web
ϕ	Conduction heat flux
ϕ_{reb}	Diameter of the rebar
θ_g	Gas temperature in the vicinity of the fire exposed element
θ_m	Surface temperature of the element
θ_r	Effective radiation temperature of the fire environment
θ	Temperature
θ_a	Temperature of the parts of the steel deck
θ_s	Temperature of the rebars in the rib
Γ	Time factor function of the opening factor O and the thermal absorptivity b
λ	Thermal conductivity
λ_a	Thermal conductivity of carbon steel
λ_{air}	Thermal conductivity of air
λ_c	Thermal conductivity of concrete
ρ	Density
ρ_a	Density of carbon steel
ρ_{air}	Density of air
ρ_c	Density of concrete
σ	Stefan-Boltzmann constant

Chapter 1

INTRODUCTION

1.1 General

A composite steel-concrete slab consists of a cold-formed profiled steel deck which acts as permanent formwork to the concrete topping. Usually, the concrete is reinforced with individual longitudinal reinforcement bars placed within the ribs and an anti-crack mesh, as illustrated in Figure 1.1 The composite action between the steel and concrete is generally achieved by indentations or embossments in the steel deck [1]

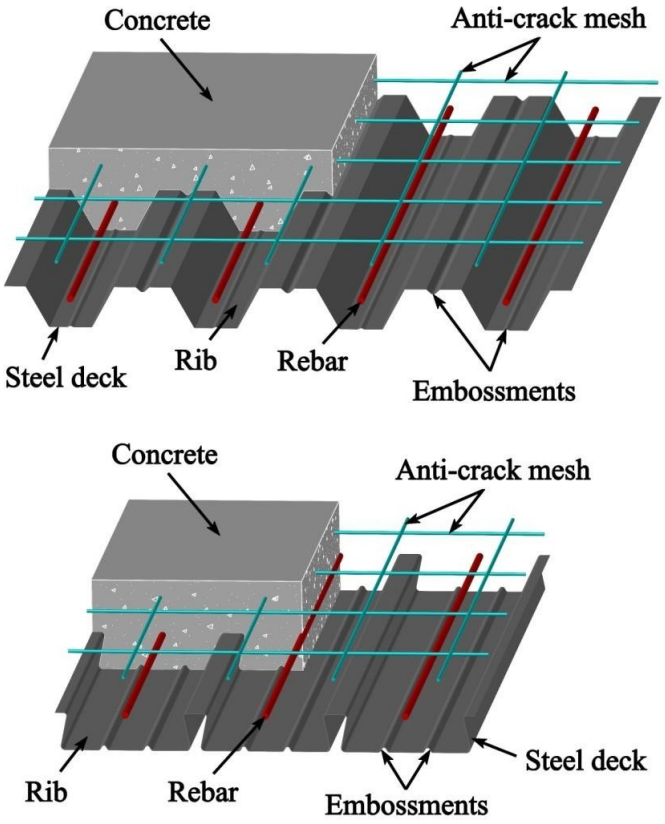

Figure 1.1: Typical layout of composite slabs trapezoidal and reentrant profiles [2]

The additional steel reinforcing elements incorporated within the concrete layer on composite slabs have several functions such as reinforcing the structure hence allow openings, distributing the effects of concentrated and linear loads, improving the fire resistance, and controlling concrete cracking [3].

The steel deck has three different functions: before concrete pouring, it acts as a work platform and safety shield; during casting, the deck serves as permanent formwork; and after hardening of the concrete, the deck serves as reinforcement [1]. Owing to the relative ease of casting concrete, trapezoidal deck slabs are more popular than re-entering ones [4].

Fire resistance of an assembly or material can be defined as the property to endure fire or protect from it. On structural engineering elements, it is measured by the time and can be associated with the capacity of confining a fire or to maintain performing the

structural function during fire exposure, or both. On composite slabs, the fire resistance is principally affected by the thickness of the steel deck, type of aggregate in concrete and the thickness of the concrete layer [4]. Several other aspects may influence the fire endurance of composite slabs such as the diameter and concrete cover for the reinforcement bars.

Large-scale fire tests on elements of construction are expensive and time-consuming. As a workaround, numerical methods can provide a rapid and cost-effective approach to problems of heat transfer and even "afford" accurate predictions of the fire performance of structures [5].

Simplified calculation methods to determine the fire resistance of composite slabs are presented by the European Standard EN 1994,Part 1.2 [6]. The calculation rules are suitable for a specific range of unprotected composite slabs with trapezoidal and re-entrant steel deck exposed to fire according to standard temperature-time curves. As you see in the figure 1.2 and 1.3

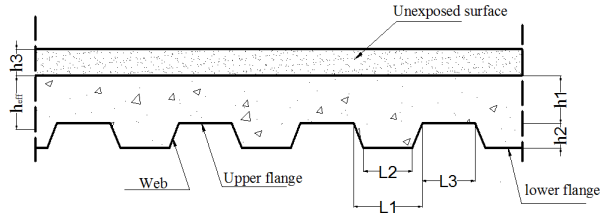

Figure 1.2: Schematization of the profile of composite slabs with trapezoidal steel deck (adapted from EN 1994,1.2 [6])

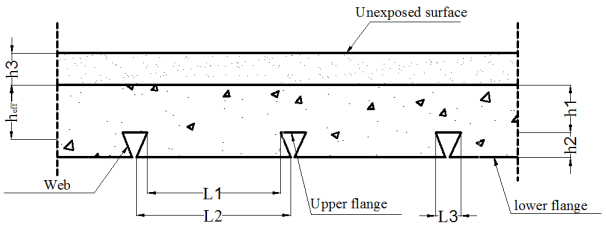

Figure 1.3: Schematization of the profile of composite slabs with re-entrant steel deck (adapted from EN1994,1.2 [6])

Previous research mentioned the separation of the steel deck from the concrete topping. Composite panels exposed to fire increase the thermal resistance of this interface (see, for example,[7]). Foundation work is focused on using different steel deck geometries, concrete thickness and other parameters to numerically simulate the fire behavior of the composite slab.

1.2 Objective

The main objective of this investigation is to find the temperature effect on the sagging moment of a composite slab with a steel deck. This study intends to present a new approximation for temperature calculation of every component used in annex D of EN1994,1.2, comparing the results from two different solution methods (simple calculation method and advanced calculation methods). Besides, the created limited component models ought to be approved against test information gave by various creators. The final goal of this work is to study the coefficients for the temperature calculation of the 4 components (three parts of steel deck: lower flange, web and upper flange and rebars). The numerical results should be compared with the simplified calculation methods of EN 1994-1-2 [6].

1.3 Motivation

The increasing use of composite structures in buildings has highlighted the need for a precise and refined analysis of the thermal and structural behaviour of these elements under fire. In this way, it is possible to adopt economical solutions while allowing safe and efficient constructions. The analytical solution of problems involving complex geometries and material properties is generally difficult and often impossible. An alternative for these cases is the application of numerical methods, namely finite element methods (FEM)

[8]. Due to the exponential growth of computing over the past decades, several FEM-based computer programs have been developed. Along with the increase in the power processing units of computers, complex engineering problems being solved through of numerical simulations using these programs. As a result, several studies have shown that numerical analysis is an effective approach to determine thermal and mechanical results. A large number of numerical simulations have provided valuable information and improved knowledge on the behaviour of composite slabs with steel decks during fire exposure. Nevertheless, the majority of these studies have focused on the structural response, using thermal analysis to provide input data for the structural model. Annex D of EN 1994,1.2 [9] presents a simplified calculation method for the calculation of the fire resistance of unprotected composite slabs subjected to the standard ISO 834 curve from below. In recent years, no revision has been made to this method and the range of geometric parameters of profiles marketed today has considerably increased compared to the range used in the decade of 1990. For these reasons, it is estimated that thermal analyses must be performed to assess the accuracy of these calculation rules. In the present investigation, it is expected that the development of the new tool for the evaluation of fire resistance, together with the results of the numerical simulations, will provide consistent data for the development of future studies. In addition, this work intends to contribute to the community by increasing knowledge about the fire behaviour of composite slabs and by promoting scientific development, thus providing increasingly safe buildings.

1.4 Organization of the thesis

The thesis is organised in to six chapters. In the following paragraphs, a brief description of the contents of each is presented.

Chapter 1 is an introduction to the research work presented in this thesis, where the objective and motivation is presented. The state of the art is also included.

Chapter 2 deals with the description of the different fire curves, modes of heat transfer, and the openness factor and experimental tests.

Chapter 3 presents the thermal properties of materials and the simple calculation method also applied to the slab when subjected to three main boundary conditions, on the lower part, the upper part, and on other regions.

Chapter 4 describes FEM principles as well as the development of both finite element models for numerical simulations using ANSYS software and the numerical validation for the different points in the slab using the model with a fixed air gap.

In Chapter 5, the description and the results of the parametric studies are outlined. A discussion around the influence of each studied parameter is also presented. The validation of the thermal models and comparisons between the outcome of the numerical simulations and Eurocode 4,Part 1.2 calculation rules are presented. Based on the general evaluation of the results.

Chapter 6 presents the main conclusions and proposals for future work.

Chapter 2

COMPOSITE SLABS UNDER FIRE

2.1 State of the art

The first reference of the application of steel deck as a structure to support a concrete floor occurs in 1920 decade. In 1926, based on the demand for new construction solutions, Loucks and Gillet developed and patented the steel deck system [10]. At that time, only the steel deck provided the structural resistance and the concrete layer was responsible to level the surface and assure fire resistance. This solution demonstrated to be more efficient than conventional reinforced concrete floors, because the steel deck worked as a permanent formwork and construction platform [11].

In the decade 1950, the first composite slab with profiled steel deck called Cofar was produced and marketed by Granco Steel Products Company, Missouri [12]. The developed composite solution consisted of a trapezoidal deck section with a mesh of cold drawn wires welded transversely across the deck troughs, associated with a concrete topping.

In 1954, Friberg [13] published the primordial expressive article about design criteria of composite slabs after numerical and experimental evaluations of the system 8 Cofar. This research provided a cost comparison between the composite system and traditional

reinforced concrete slabs. The results of the tests demonstrated good agreement with what was expected and it was observed that this solution had similar structural resistance in comparison with similar reinforced concrete slabs. With the objective to avert the use of welded mesh and assure horizontal shear transfer between the steel and concrete to achieve composite action, a new steel deck profile with embossments and re-entrant parts was developed by Inland-Ryerson.

The company HiBond in 1961 [10], introduced, the new trapezoidal profile and was the forerunner of modern profiled steel decks for composite slabs that use indentations as a mechanism of shear transference [6]. The first concept of "fire engineering" applied to steel.

Structures was introduced by Petterson et al.[14] in 1976. The publication exposes principles, which govern rational fire engineering design, comparisons between suspended ceilings carrying floor slabs of lightweight concrete under fire exposure conditions and a description of prevailing materials and methods used for structural fire insulation. In Europe, the use of composite steel-concrete structural components increased significantly in the decade of 1980. Until this time, the structural fire resistance was calculated mostly by experimental tests, which are substantially expensive and time-consuming [15]. In 1983, recognizing the need for a calculation method, the ECCS (European Convention for Constructional Steel work) [16] published the first instructions for the practical design of composite slabs under fire conditions. This technical note introduced simple calculation methods based on criteria for fire resistance of the standard ISO 834 [17], hence inspiring the diffusion of the use of composite slabs.

Between 1983 and 1985, the Construction Industry Research Information Association (CIRIA) performed a test program sponsored by the dominant steel deck manufacturers in the United Kingdom. The fire tests were conducted on one large-scale and on five smaller-scale loaded composite slabs with reinforcement meshes. The investigation indicated that design recommendations were generally conservative and the slabs with dovetail profiles normally presented better fire resistance in comparison to slabs with trapezoidal profiles, among other conclusions [9].

In parallel, between the years of 1984 and 1986, with the support of the Fire Research Station (FRS), the British Steel Corporation (BSC) developed a test program on three different large-scale specimens. The research consisted of loaded fire tests 9 carried out on continuous composite slabs with welded bars as reinforcement. From the results of the tests, it was concluded that some requirements for minimum slab depth were too conservative and several cautions must be taken concerning the use of high tensile drawn reinforcement due to the breaking of some bars over the supports during the tests [9].

H. D. Wright et al [18] (1987) authors have studied the efficiency of m-k tests to carried out m-k bending tests and push out on two types of sheeting, trapezoidal and re-entrant shapes in both transverse and longitudinal direction. The concrete strength varied from $25N/mm^2$ to $55N/mm^2$. It is concluded the increasing the height of embossment increases the load bearing capacity and even the weakest concrete showed the same load bearing capacity.

W. Samuel Easterling et al [19] (1992) developed a new method to determine the strength and stiffness of the composite slabs. Six composite slabs were cast. One of the specimens is three spans continuous. Both the analytical and experimental results were compared that indicates that proper anchorage should be provided at the ends of the deck sheets if ductility is to be obtained. The tests method described in the ASCE specifications does not accurately predict since it does take the influence of adjacent slabs.

Pentti and Sun [20] (1999) studied the shear-connection behaviour of composite slabs with particular profiled steel sheeting. Twenty-seven push-out tests specimens of different shapes, sizes, locations of embossments and different steel sheeting thicknesses were carried out in two test series. It is concluded that increasing the embossment depth, length, thickness have a significant increase in shear stress. Among these three parameters embossment depth plays a vital role.

Matthew J. Burnet and Deric J. Oehlers [21] (2001) developed a new form of push-out test that simulates the bond characteristics more accurately and where 33 tests were developed to determine the main parameters that affect both the chemical bond and State of Art on Composite Slab Construction 3 mechanical bond strengths of dovetailed

and trapezoidal rib shear connectors. All the specimens are governed by the ratio of the breadth of the rib to the breadth of the flange. Embossments were found to have a relatively minor effect on specimens with small values of the breadth of the rib to the breadth of flange ratios such as occurs in dovetailed sections and have substantial effects on specimens with large values of the breadth of the rib to breadth of flange ratio as occurs in trapezoidal specimens.

S.Chen [22] (2003) carried out experiments on seven simply supported one-span composite slabs and two continuous composite slabs to identify the shear-bond action in composite slabs. Different end restraints have been used in the simply supported slabs. The slabs with end anchorage of steel shear connectors were found to bear higher shear-bond strength than that of slabs without end anchorage.

Miquel Ferrer et al [23] (2006) concluded from the finite elemental analysis that: (1) minimum retention angle should be provided, (2) alternate directions of embossments (inwards and outwards) tilting are not effective, (3) too steep embossments are dangerous, (4) embossment length should be large and better if located near the edges and 5 embossment spacing should be minimum.

In the same year G. Marciukaitis et al [24] (2006) describes that when a load is applied to composite slabs the connection between steel profiled sheeting and the concrete is not stiff and there are cracks in the tension zone of the concrete layer. Therefore, when calculating deflections for such slabs, it is necessary to consider the partial stiffness of the connection between layers, the effect of normal cracks in the concrete layer, and the plastic deformations of compressed concrete for the stiffness of this layer.

V. Marimuthu et al [25] (2007) have conducted experimental investigations on 18 composite deck slabs by varying the shear spans and found that, the behaviour of the embossed profiled composite steel deck slab depends mainly on the shear span. For the shorter shear spans, strength of the slab is governed by shear bond failure, and for large shear spans by flexural failure Youn-Ju Jeong [26] (2008) developed a model based on the partial interaction from the results of push-out tests. It suits well with the results obtained from m-k method, which requires full-scale slab specimens. The state of start

shows that it serves as a better way for partial interaction studies.

Melchor Lopez Ávila et al [27] (2009) carried out Pull out tests and a numerical model using abaqus was developed. Considering the good agreement between the numerical and experimental results, concluded that the hypotheses adopted in the numerical model are correct, which guaranteed that the physical phenomenon of the problem could be reproduced in particular the longitudinal sliding.

Redzuan Abdullah and Samuel Easterling [28] (2009) found a new procedure referred to as the Force Equilibrium method for calculating the shear bond in composite slabs from bending test data. The procedure was used to produce the shear bond end slip relation, which is useful for numerical analysis.

Noémi Seres–László Dunai [29] (2011) introduced a new test specimen to analyse the local behaviour of embossments contrary to traditional experimental methods, which take smeared mechanical bond into consideration. An experimental investigation of an individual embossed mechanical bonds is detailed. The change of the plate thickness has direct effect on the initial stiffness and the load bearing capacity. The results are used for the validation of the developed finite element model for the embossment behaviour.

Baskar R. [30] (2012) studied the strength and behaviour of composite slabs both experimentally and analytically. Ten composite slabs were cast based on embossments, and embossments and end anchorages, without embossments. Both the experimental and analytical results were comparable. The load ratio between experimental and finite elemental values for without embossments, and with embossments, with embossments and end anchorages groups were 1.02, 1.09, 1.16.The load bearing capacity of the slabs with embossments and end anchorages groups was found to be greater among the two. Embossments play a vital role in increasing the longitudinal shear capacity of slabs.

J. Holomeka and M. Bajera [31] (2012) carried out four-point bending tests, vacuum loading and small scale shear tests. They concluded that small-scale tests represent an interesting alternative to expensive and time-consuming four-point bending tests, which are required in current standardized design methods. The disadvantage is that they cannot include all the properties influencing the longitudinal shear resistance of composite slabs.

Small-scale test set up can significantly influence the results; however the setup is not described in any standard.

Namdeo Adkuji Hedaoo et al [32] (2012) casted a total of 18 full-scale composite slab specimen and tested to determine (1) the structural behaviour and (2) the load-bearing capacity. For the partial shear connection method, analysis is based on actual measured strengths, and hence, it indicates a very small difference between actual failure load and design load. The m-k method results are weaker than the experimental method by 43%. This difference occurred since the design load values for m-k method are based on regression values reduced by 10% and the use of λ_{vs} of 1.25. From the design perspective of the composite slabs, partial shear connection method will give optimum design as compared to m-k method.

K. N. Lakshmikandhan [33] (2013) investigated experimentally three types of mechanical connector schemes. Three mechanical shear connector schemes develop full a shear interaction and do not show any visible delamination and slip. The inclusion of shear connector enhances the flexural capacity, stiffness, ductility, and energy absorption of the composite deck system. The flexural capacity of composite deck the slab with wire mesh is found competitive for shrinkage and temperature effects.

Héctor Cifuentes and Fernando Medina [34] (2013) considered two different types of profiled steel sheeting with up to three different thicknesses. This involved testing 30 State of Art on Composite Slab Construction 5 composite slabs with different experimental requirements. The thickness of the steel deck was an important parameter regarding the longitudinal shear strength of composite slabs. The experimental results obtained improved significantly with the increase of steel deck thickness, especially in long-span specimens.

R.P. Johnson and A.J. Shepherd [35] (2013), mentioned, a design method allowing for the additional resistance to longitudinal shear given by reinforcing bars parallel to the ribs of the sheeting (also increasing fire resistance). The tests and analyses reported here confirm the use of the simpler linear version of this method with the usual partial factors for the materials and shear resistance.

A. Gholamhoseini,[36] (2014) studied the longitudinal shear capacity of four types (two trapezoidal and two re-entrant)of profiled decking that are widely used in Australia, by using full-scale load tests. The ultimate shear stress for each type of slab tested at the shear span of (L/6) was greater than that obtained when the shear span was (L/4), being L the clear span of the testing specimen in millimetres. A finite element model utilizing interface elements to model the bond properties between steel decking and concrete slab is described and used to investigate the behaviour of the slabs throughout the full range of loading.

U. Shah [37] (2014) modelled composite slabs using ANSYS by varying thickness, with and without embossments. He concluded that the thickness of the profile sheet has a considerable effect on the deflection and stress of the composite slab. Comparing the solution without embossments and with embossments, it is observed that the solution with embossment composite slab has less deformation by almost 34% to 41% and less stress by almost 26% as the thickness is increased from 0.9 mm to 1.2 mm. Thickness of the steel deck plays a significant role.

In 2017, Jiang et al [38] from the National Institute of Standards and Technology (NIST) presented a numerical study based on detailed and reduced-order models of heat transfer in composite slabs. Two-dimensional thermal analyses were performed using the LS-DYNA finite-element software. The main objective of this research was to develop a reduced-order modelling approach applicable for both thermal and structural analysis, in order to simplify the analysis of the structural behaviour under fire conditions. Solid elements were used for the concrete slab and shell elements for the steel deck. Both detailed and reduced-order models were validated against experimental tests and a parametric study using the detailed model was conducted to evaluate the effect of some parameters on temperature development such as thermal boundary conditions, thermal properties of materials, and slab geometry. In addition, the specific heat of the concrete was modified to better estimate the heat input in the web, and thereafter an equation for the modification was suggested. In order to consider the effects of the change in emissivity of the galvanized steel deck due to the melting of the zinc layer, a novel method to calculate

the temperature-dependent emissivity was proposed. Generally speaking, it was observed that satisfactory results did not require a great refinement of the finite element mesh and temperatures at the unexposed side were mainly affected by the thickness of the concrete topping. The results of the proposed model for emissivity showed better agreement with experimental results than those calculated from the standard EN 1994,1.2 [6].

In 2018, an investigation of the thermal performance of composite slabs under standard fire conditions was directed by Prates [2]. The critical target of this study was to foster two-layered mathematical models utilizing the product MATLAB and ANSYS to assess the imperviousness to fire of various piece setups as per the protection rule. A few mathematical recreations were performed to examine the impact of both concrete and steel deck thicknesses on the unexposed side temperature. Taking into account that the thermal conductivity isn't affected by the mechanical way of behaving, trial fire tests were led on two unloaded samples. Additionally, the aftereffects of mathematical reenactments were contrasted against the outcomes got and the exploratory tests as well as the improved technique given in EN 1994,1.2 [6] and NBR 14323 [39]. The imperviousness to fire got from the mathematical models was extensively more modest than those deliberate on the trial tests and an examination between the mathematical and worked on technique results confirmed that the plan rules appear to be perilous assuming an ideal contact is considered for the high-level computation technique. As per the mathematical outcomes, a new and better guess was proposed

In 2019, Jian Jiang et al. [42] conducted a numerical investigation around different parameters that may influence the fire resistance of composite slabs concerning to the thermal insulation criterion (I). An improved algebraic expression for the calculation of the fire resistance that explicitly accounts for the moisture content of concrete was proposed. The formulation is applies to an extended range of geometries in comparison to the limitations of the calculation method presented in the current version of Eurocode 4. A set of 54 composite slabs was selected for numerical analyses using a high-fidelity finite element approach. It was concluded that the concrete thickness and the moisture content were the parameters that most influenced the fire resistance. The proposed expression for

fire resistance was validated against additional analyses and experimental data, resulting in maximum deviations of 15 and 18 minutes, respectively.

In 2019, Piloto et al.[43] [44] [45] [46] carried out numerical research concerning the fire behaviour of composite slabs under standard fire conditions. The main objective of this investigation was to evaluate the fire resistance of this structural element from the thermal insulation standpoint. Three-dimensional thermal models were implemented using ANSYS and MATLAB PDE toolbox, considering slabs with perfect thermal contact between all materials, and an insulating layer with a constant thickness (air gap) between the steel deck and the concrete topping to simulate debonding effects. It was concluded that the perfect contact model underestimates the fire resistance (I) and the results of the air gap model present good agreement with experimental results. Further research was conducted by the authors [47] with the aim to propose an improved method for the estimation of the temperature of the parts of the steel deck and the rebars of composite slabs subjected to standard fire exposure. It was observed that the assessment rules given in the EN 1994 – 1-2 for the temperature of the steel components of composite slabs were generally on the unsafe side and do not consider important parameters.

In the year of 2020 Juan José del Coz-Díaz,Juan Enrique Martínez-Martínez [48] developed an investigation of the experimental study of lightweight concrete (LWC) and normal weight concrete (NWC) composite slabs with steel decking profile exposed to standard time-temperature curve. In this study, the fire behaviour of NWC is compared with the fire behaviour of LWC composite slabs. Dimensions of the slab are 160 mm thick, 1120 mm wide and 2030 mm long. In order to perform fire tests in the intermediate-scale samples, a non-standard furnace was designed and assembled. The furnace is composed of a heating chamber, an exhausting system and a portal frame. The heating chamber is made of a steel framework and refractory layers. The exhausting system, which has an auxiliary vein with a fan to introduce air, is responsible to extracts hot gases. The portal frame is composed of steel profiles with a rotating beam equipped with a linear actuator to apply the load on the samples. This beam is opened to allow the slabs to be placed and closed during the test.

In 2020 Paulo AG Piloto, Carlos Balsa [49] Conducted an investigation, where a new advanced calculation method is presented, using the software ANSYS. The numerical model is first validated with experimental data reported on the literature and then a parametric analysis is conducted to better understand the effect of the load level on the composite structure under fire. The validation of the simulations consisted of three different models: the first model considers perfect contact between the steel deck and the concrete topping, and the two following models consider the existence of an air gap between these materials, acting as a thermal resistance on the temperature field through the thickness of the slab. The numerical results show good agreement to the experimental results, mainly when using the non-perfect contact model, reaching 3.88% and 16.91% of difference concerning to the insulation and load-bearing criteria, respectively. Based on the validation models, a parametric study is presented, modifying the load level from 10% up to 75%. New simple calculation models are presented to define the fire resistance of composite slabs, considering the load level, and the debonding effect between the concrete and the steel deck.

In 2021 Bolina,et al. [50] studied the temperature distribution in the cross-section of steel decking concrete slabs subjected to fire using three different solution three different procedures:(a) experimental,(b) numerical and (c) analytical methods. The experimental tests corresponding to eight real scale fire tests on slabs were developed by the authors. These tests have been used to calibrate numerical models for being used with the finite element software Abaqus. The analytical methods were the ones proposed in Annex D of EN 1994-1-2. The analytical steel decking temperatures showed convergence with the experimental and numerical ones. The same was not observed for the concrete, positive and negative rebar, and thermal insulation temperatures.

2.2 Fire safety

Fire has always been a very destructive accidental phenomenon. The fire risk will always exist because of fire accidents and it is impossible to use only incombustible

products in buildings. The primary goal of fire protection is to limit the probability of death and reduce the loss of the property. The most common objective in providing life safety is to ensure safe escape by giving time to people before the collapse of the building. To do this, it is necessary to use more fire-resistant materials in construction and protect the structural elements. Finally it is important to alert people to provide suitable escape paths and ensure that they are not affected by fire or smoke while escaping through those paths to a safe place. According to the Portuguese regulation [51] and fire resistance criteria are: Insulation (I), Integrity (E), and load-bearing capacity (R) depending on the type of structural elements, buildings must have (REI) Integrity (E) and insulation (I). The load-bearing capacity (R) is the time in completed minutes for which the test specimen continues to maintain its ability to support the test load during the experimental test satisfying well-defined performance criteria. The integrity (E),represents the time in completed minutes for which the test specimen continues to maintain its separating function during the test without letting flames go through the specimen satisfying a well-defined performance criterion. The insulation is the time in completed minutes for which the test specimen continues to maintain its separating function during the test without developing high temperatures on its unexposed surface satisfying a well-defined performance criterion.then this implies that the (R30.R60.R90.R120) composite slab give the prescribed fire protection ability (for 30 or 60 or 90 or 120 minutes) and that each of the products from which consist composite slab fulfil the in pursuance of the stated class designation prevailing reaction to fire requirements on material related level. Table 2.1 below presents the fire rating for each building class (I to XII) and risk class (1st to 4th)

CLASS OF BUILDING	RISK CLASS				ELEMENT TYPE
	1^a	2^a	3^a	4^a	
I, III, IV, V, VI, VII, VIII, IX, X	R30	R60	R90	R120	SUPPORT
	REI30	REI60	REI90	REI120	SUPPORT AND PARTITIONING
II, XI, XII	R30	R60	R90	R120	SUPPORT
	REI30	REI60	REI90	REI120	SUPPORT AND PARTITIONING

Table 2.1: Minimum fire ratings for structural elements of buildings

Where the class of building is defined as:
Type I stands for residential; Type II stands for parking places; Type III stands for business buildings; Type IV stands for schools; Type V stands for hospitals and elderly homes; Type VI stands for public shows and meetings; Type VII stands for hotels and restaurants; Type VIII stands for commercial and transport station; Type IX stands for sports and leisure; Type X stands for museums and art galleries; Type XI stands for libraries and archives and finally Type XII stands for industrial and warehouse.

Where the risk class of building depends the height of the building and on the number of floors below the reference level, see Table 2.2

RISK BUILDING CATEGORY	height of buildings h	Number floors below reference n
1	9	1
2	28	3
3	50	5
4	50	5

Table 2.2: Risk building category

2.3 Fire curves

2.3.1 Nominal fire curves

The Standard temperature-time curve ISO 834 [52], also known as the Cellulosic curve and/or the standard nominal fire curve, is used as a test method determine the fire resistance of various elements of construction when subjected to standard fire exposure conditions. The test data thus obtained will permit subsequent classification based on the duration for which the performance of the tested elements under these conditions satisfies specified criteria. In 1981, Margaret Law [53] presented a summary of novel work that she and her colleagues at Arup Fire had completed to evaluate the structural fire safety of innovative and architecturally exciting buildings – such as the Pompidou Centre in Paris. Among the many topics covered in this paper, stated a number of criticisms of the standard fire resistance test and proposed the way forward using knowledge-based analytical approaches.

The standard temperature-time curve is not representative of a real fire in a real building. Indeed it is physically unrealistic and actually contradicts the knowledge from fire dynamics. The standard temperature-time curve is given according to next expression and represented in the Figure 2.1

$$\theta_g = 20 + 345 \cdot log_{10}(8t + 1) \quad [^{\circ}C] \tag{2.1}$$

Where θ_g is the gas temperature in the fire compartment [°C], t is the time [min], assuming the coefficient of heat transfer by convection equal to $\alpha_c = 25$ $[\frac{W}{m^2K}]$

2.3.2 Natural Fire curve

In real natural fire models, the complete process by fire development can be described as being composed by four different stages, see Figure 2.2 . Not necessarily all fires follow this curve, because in some situations they may disappear naturally or do not reach flashover, mainly if the fuel materials are isolated or if there is not enough air to maintain

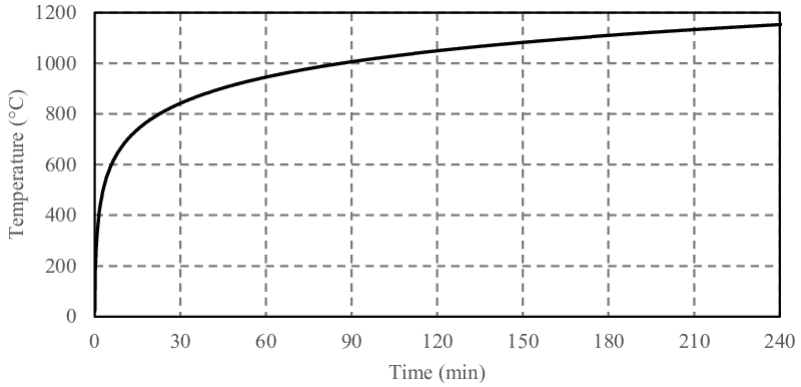

Figure 2.1: Nominal time temperature fire curves

the combustion [54]

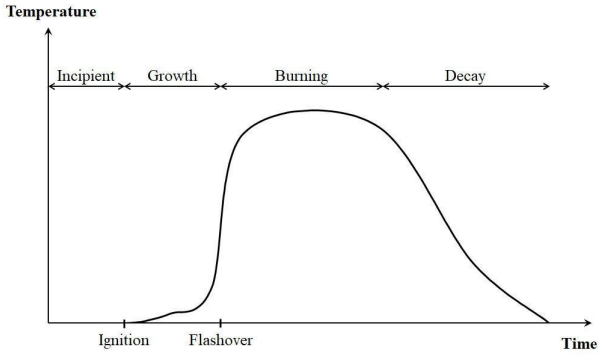

Figure 2.2: Fire curve for the complete process of fire development [54]

The initial stage is characterized by the heating of potentially combustible materials. The transition from the initial stage to the growth stage is called ignition, representing the start of combustion. In the growth stage, most fires spread slowly on the available combustible surfaces, and then more rapidly, as long as the fire grows, and there is radiant feedback from flames to other fuel materials. The flash over represents the transition from the growth stage to the burning period, characterized by a rapid increase in the burning rate. In the burning period, the temperatures and the radiant heat flux within the compartment are of such a level that all exposed surfaces are burning. Finally, after all the fuel materials in the environment have burned out, the temperatures drop and the fire load density dies in the decay period [54].

These curves may be determined from experimental fire tests in compartments using real fire conditions and present an ascending segment (heating phase), and a descending segment (cooling phase). Results of tests evidenced that the parameters that most influence on the shape of the natural fire curves are the level of fire and ventilation, as well as the thermal properties of the materials of the compartment wall [55].

2.4 Heat transfer and thermal actions

In order to better comprehend the mechanisms of heat transfer, it is necessary to make clear some basic concepts. "Temperature" can be defined as the measure of the amount of kinetic energy present in the molecules of a given substance. In other words, it is a measure of the coldness or warmth of a substance. Çengel and Ghajar [56] define "heat" as the form of energy that can be transferred from one system to another as a consequence of temperature difference.

A thermodynamic analysis deals with the amount of heat transfer as an energy system undergoes a process from one equilibrium state to another. Heat transfer is the science that concerns the determination of the rates of these energy transfers. The heat transfer between two substances requires the existence of temperature differences and occurs from the high-temperature medium to the lower-temperature medium [56].

There are three different modes of heat transfer: conduction, convection and radiation. The temperature distribution in a system depends on the combined effects of these three modes of heat transfer [55].

In order to calculate the rate of temperature increase in structural components, it is fundamental to determine the amount of heat that affects these components. The Eurocode 1 – Part 1-2 [57] presents thermal actions for temperature analysis, which are given by the net heat flux h_{net} (W/m_2) to the boundary surface of the element. On the fire exposed surfaces, the net heat flux is divided into two components: the first considers heat transfer by convection $(h_{net,cv})$ and the second by radiation $(h_{net,r})$, as presented below.

$$h_{ned} = h + h_{net,r} \tag{2.2}$$

The following subsections present the formulation used to determine each component of the equation above and give a brief description of the three modes of heat transfer.

2.4.1 Conduction

Conduction can be characterized as the exchange of energy in the body from particles of higher energy level (higher temperature) to particles of lower energy level (lower temperature) because of the cooperation between particles [56]. Conductive hotness move can happen in solids, gases, or fluids. This peculiarity is represented by Fourier's law of hotness conduction, presented in 1822. As indicated by this regulation, the conduction heat motion h_{cd} (W/m^2) is straightforwardly relative to the temperature inclination toward the progression of hotness $\frac{d_T}{d_x}$ (K/m), as introduced in condition 2.3:

$$h_{cd} = -\lambda + \frac{d_T}{d_x} \tag{2.3}$$

In the last condition, λ addresses the warm conductivity (W/mK), which is a proportion of the capacity of the material to lead heat. As expressed previously, the hotness is moved from the higher temperature particles to the lower temperature particles, bringing about a negative temperature variety toward the hotness stream. In such manner, the negative sign is important on the grounds that the heat flow in the positive x bearing is a positive worth. The conduction heat flow is a vector amount (h_{cd}), along these lines, in the three-layered space, this part can be composed as:

$$h_{cd} = -\lambda \cdot (\delta x, \delta y, \delta z)^T \cdot T \tag{2.4}$$

In the equation above, the vector derivative is the gradient operator (Δ) applied to the temperature T.

2.4.2 Convection

Convection heat transfer is characterized as the method of energy transfer between a solid surface and a liquid (fluid or gas) in development on its limits, including consolidated impacts of conduction and smooth movement. The more prominent the speed of the liquid is, the more noteworthy the convection heat move. Whether there is no mass smooth movement, the heat transfer between the solid and nearby liquid is administered by conduction [56].

The convection heat transfer is the energy that is transferred between a solid and a moving fluid or gas, each being at different temperatures. The rate at which this exchange of energy occurs is given by Newton's law of cooling, shown equation 2.5:.

$$h_{net,cv} = \alpha_{cv} \cdot (\theta_g - \theta_m) \tag{2.5}$$

Where, α_{cv} is the coefficient of heat transfer by convection (W/m^2K), relevant for nominal temperature-time curves; θ_g represents the gas temperature in the vicinity of the fire exposed element ($^\circ C$); and θ_m is the surface temperature of the element ($^\circ C$). The convection coefficient value depends on the velocity of the fluid or gas and should be considered equal to $\alpha_{cv} = 9$ (W/m^2K),$\alpha_{cv} = 25$ (W/m^2K) and $\alpha_{cv} = 50$ (W/m^2K) for cases of non-exposed surface, exposed surface with ISO834 curve and exposed surface with hydrocarbons.

2.4.3 Radiation

Radiation comprises of the energy transmitted by issue as electromagnetic waves (photons) because of changes in the electronic arrangements of particles or atoms. Contrary to conduction and convection, this convection, this method of hotness move doesn't need a material medium, that is to say, the hotness can likewise be moved through locales of vacuum [56].

The greatest measure of warm radiation E_b (W/m^2) which can be produced from a not entirely settled by the Stefan-Boltzmann regulation. This regulation expresses that

a glorified surface called blackbody (optimal warm radiator) transmits warm radiation relative to the fourth force of the outright temperature $T(K)$, as given underneath.

$$E_b = \sigma \cdot T^4 \tag{2.6}$$

In Eq 2.6 σ is a proportionality constant called Stefan-Boltzmann constant, which is equal to $5.67E-8$ (W/m^2K^4). This equation is suitable only for radiation emitted by a blackbody, which is of fundamental importance to radiant heat transfer [59].

The radiation produced by genuine surfaces should think about an extra component. This component is called emissivity ϵ, which is a worth somewhere in the range of 0 and 1 characterized as the proportion of the energy transmitted by the genuine surface to the energy discharged by a blackbody, both at a similar temperature [60]. For an overall surface, the complete brilliant transmitted energy E (W/m^2) can be communicated as:

$$E_b = \epsilon \cdot \sigma \cdot T^4 \tag{2.7}$$

For disentanglement purposes, whether the emissivity is free of these variables, As per Eurocode 1, Section 1-2 [57] and considering the ideas introduced over, the net radiative heat flux part $h_{net,r}$ (W/m^2) for temperature investigation of structural individuals ought not to set in stone as per the following equation.

$$h_{net,r} = \phi \cdot \epsilon_m \cdot \epsilon_f \cdot \sigma \cdot ((\theta_r + 273)^4 - (\theta_m + 273)^4) \tag{2.8}$$

In the last equation 2.8, (dimensionless) is the view factor, which takes into consideration position and shadow effects, ϵ_m (dimensionless) represents the surface emissivity of the element; ϵ_f (dimensionless) represents the emissivity of the fire; σ is the Stefan-Boltzmann constant (W/m^2K^4), θ_r is the effective radiation temperature of the fire environment $(^\circ C)$; and θ_m is the surface temperature of the element $(^\circ C)$

The emissivity of the material for steel and concrete is equal to 0.7.The emissivity of the fire (flames) is assumed to taken as 1.and the view factor can be assumed equal to

1,0 when not specified.

In the numerical modelling acted in this examination, the gas temperature is thought to be the compelling radiation temperature of the fire climate, approximated by the Stefan-Boltzmann regulation. In this way, considering convection and radiation heat flux, the net heat flux, which influences a primary part enduring an onslaught conditions can be composed as:

$$h_{net} = \alpha_{cv} \cdot (\theta_g - \theta_m) + \phi \cdot \epsilon_{res} \cdot 45.67E - 8 \cdot [(\theta_r + 273)^4 - (\theta_m + 273)^4] \tag{2.9}$$

In the equation above, ϵ_{res} (dimensionless) represents the resulting emissivity, which is the product between the surface emissivity of the member and the emissivity of the fire.

View factor

The view factor Φ for composite slabs with a steel deck from the place of fire to the lower part of the steel deck is by and large taken as solidarity. For composite slabs with profiled trapezoidal or reentrant, it relies upon the direction of surfaces and the distance between them. Because of the check from the trap of steel deck (the slanted piece of the Figure 2.3 Math for the assurance of view factor between two surfaces), This approach is additionally taken on by the guidelines EN 1994,1.2; in any case, this report just gives the articulation for the upper rib.

The view factor of the lower flange of composite slabs is given as $\Phi_{low} = 1$. Inferable from the check to coordinate openness brought about by the ribs of the steel deck, the view factor of the web and upper flange are more modest than one. These view factor can be determined following the basic crossed-strings strategy (see Figure 2.3), created by H. C. Hottel during the 1950s [56]. This approach is additionally embraced by the principles EN 1994,1.2; notwithstanding, this report just gives the articulation for the upper rib.

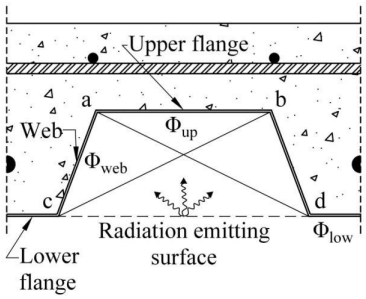

Figure 2.3: Schematic for the calculation of the view factor [51])

The view factors of the upper flange (ϕ_{up}) and web (ϕ_{web}) can be determined through the distances between the pieces of the steel deck or by utilizing the mathematical boundaries of the composite slabs. The articulations for the computation of these view factors of composite slabs with either trapezoidal or re-contestant profiles are introduced in Eqs. 2.10 and 2.11.

$$\phi_{up} = \frac{\sqrt{h_2^2 + (l_3 + \frac{l_1 + l_2}{2})^2)} - \sqrt{h_2^2 + (\frac{l_1 + l_2}{2})^2}}{l_3} \tag{2.10}$$

$$\phi_{up} = \frac{\sqrt{h_2^2 + (l_3 + \frac{l_1 + l_2}{2})^2} - \sqrt{h_2^2 + (\frac{l_1 + l_2}{2})^2} - (l_3 + l_1 - l_2)}{l_3} \tag{2.11}$$

Chapter 3

THERMAL PROPERTIES OF MATERIALS

3.1 Concrete

The specific heat of concrete varies mainly with the moisture content. The moisture within the concrete causes a peak between 100 [°C] and 200 [°C] due to the water being driven off. Figure 3.1 depicts the variation of this property with temperature. The pick value depends on the amount of moisture, in this case u = 3% was assumed. The Eurocode EN 1992,1.2 [61] recommends the following relationship for calculation of concrete specific heat.

$$20\ \ (^{\circ}C) \leq \theta \leq 100\ \ (^{\circ}C) \quad C_P(\theta) = 900 \tag{3.1}$$

$$100\ (^{\circ}C) \leq \theta \leq 115\ \ (^{\circ}C) \quad C_P(\theta) = 2020 \tag{3.2}$$

$$115\ (^{\circ}C) \leq \theta \leq 200\ \ (^{\circ}C) \quad C_P(\theta) = 2020 - \tfrac{\theta-115}{12} \tag{3.3}$$

$$200\ (^{\circ}C) \leq \theta \leq 400\ \ (^{\circ}C) \quad C_P(\theta) = 100\ - \tfrac{\theta-200}{2} \tag{3.4}$$

$$400\ (^{\circ}C) \leq \theta \leq 1400\ (^{\circ}C) \quad C_P(\theta) = 1000 \tag{3.5}$$

In the equations above, cp is the specific heat of dry concrete (J/kgK), and θ is the concrete temperature (°C).

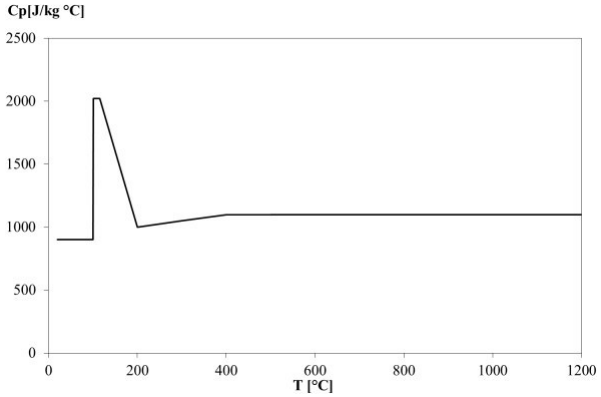

Figure 3.1: Specific heat at elevated temperature [61]

The thermal conductivity depends upon the aggregate type and the temperature of the concrete. The thermal conductivity λ_c of concrete may be determined between lower and upper limit values. Fig. 3.2 represents the variation of the upper limit of thermal conductivity with temperature. The following equation defined in Eurocode EN 1992,1.2 [42] recommends the upper limit for normal-weight concrete. θ is the concrete temperature (°C).

$$\lambda_c = \frac{(2 - 0.2451) \cdot \theta}{100} + (\frac{0.0107 \cdot \theta}{100})^2 \qquad [\lambda_c(W/mk] \tag{3.6}$$

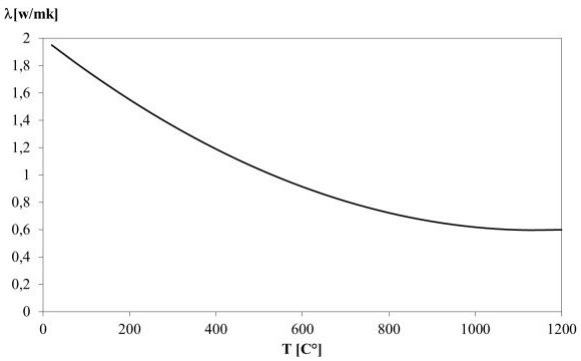

Figure 3.2: Thermal conductivity at elevated temperature [42]

The density is a physical property of matter, qualitatively it is defined as the heaviness of objects with a specific volume, and is denoted by ρ. Common unit of density is (kg/m^3). Fig.3.3 represents the variation of density with temperature. The reference value for density at room temperature has been considered $\rho(20°\text{C}=2300\ (Kg/m^3)$, The Eurocode EN 1992,1.2 [61] recommends the following relationship for the calculation of concrete density.

$$20\ \ (°C) \leq \theta \leq 115\ \ (°C) \quad \rho(\theta) = \rho(20°C) \tag{3.7}$$

$$115\ (°C) \leq \theta \leq 200\ \ (°C) \quad \rho(\theta) = \rho(20°C) \cdot \frac{1-0.02\cdot(\theta-115)}{85} \tag{3.8}$$

$$200\ (°C) \leq \theta \leq 400\ \ (°C) \quad \rho(\theta) = \rho(20°C) \cdot \frac{0.98-0.03\cdot(\theta-200)}{200} \tag{3.9}$$

$$400\ (°C) \leq \theta \leq 1200\ (°C) \quad \rho(\theta) = \rho(20°C) \cdot \frac{0.95-0.07\cdot(\theta-400)}{800} \tag{3.10}$$

In the equations above, $\rho_s\ (\theta)$ is the density of concrete (kg/m3) and θ is the concrete temperature (°C). The relationship between temperature and concrete density is shown graphically in Figure 3.3.

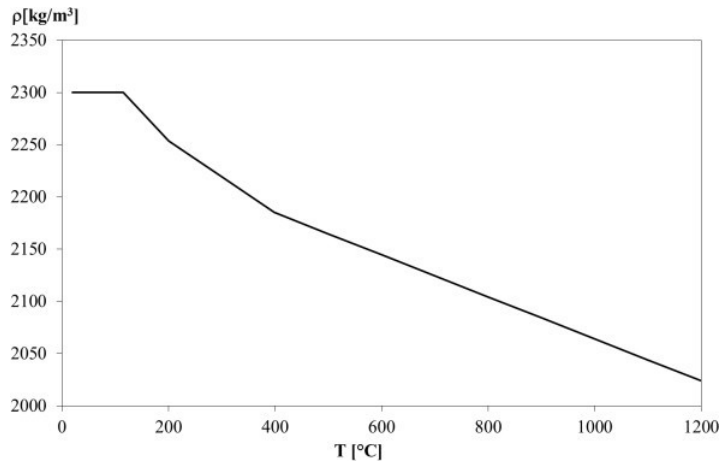

Figure 3.3: Density of concrete at elevated temperature [61]

3.2 Carbon steel

The Specific heat of steel represents the amount of energy that is necessary to raise the unit mass of steel temperature by 1[°C], it is also the measure of the materials ability to absorb heat. The specific heat of steel "Ca" is defined in accordance to Eurocode EN1993,1.2 [62] as the following:

For $20°C \leq \theta \leq 600°C$

$$C_a = 425 + 7.73 \times 10^{-1} \cdot \theta_a - 1.69 \times 10^{-3} \cdot \theta_a^2 + 2.22 \times 10^{-6} \cdot \theta^{-3} \tag{3.11}$$

For $600°C \leq \theta \leq 735°C$

$$C_a = 666 + \frac{13002}{738 - \theta_a} \tag{3.12}$$

For $735°C \leq \theta \leq 900°C$

$$C_a = 545 + \frac{17820}{\theta_a - 731} \tag{3.13}$$

For $900°C \leq \theta \leq 1200°C$

$$C_a = 650 \tag{3.14}$$

In the equations above, θ_a is the steel temperature (°C). The variation of the specific heat of carbon steel with temperature is presented in Figure 3.4.

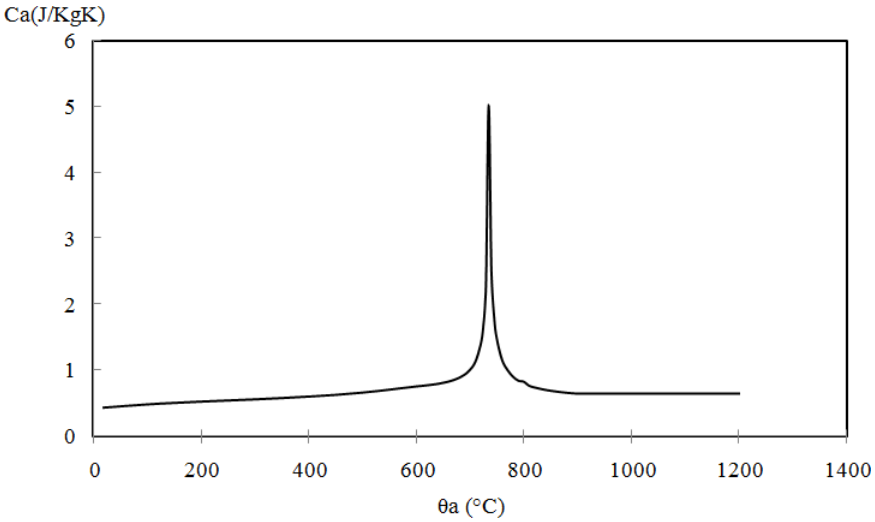

Figure 3.4: Variation of the specific heat of carbon steel with temperature [62]

Thermal conductivity is the coefficient which dictates the rate which heat arriving at the steel surface is conducted through the material. According to Eurocode EN1993,1.2 [62] the variation of thermal conductivity with temperature is represented in Fig 3.5. The thermal conductivity of steel λ_a should be determined from the following:

For $20°C \leq \theta \leq 800°C$

$$\lambda_a = 54 - 3.33 \times 10^{-2} \tag{3.15}$$

For $800°C \leq \theta \leq 1200°C$

$$\lambda_a = 27.3 \tag{3.16}$$

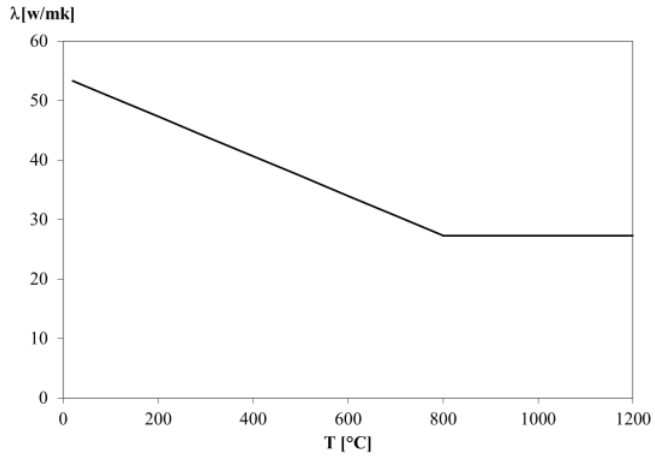

Figure 3.5: Thermal conductivity at elevated temperature [62]

The density of steel is constant $\rho = 7850\ kg/m^3$, even when the temperature is modified. According to Eurocode EN1993-1-2 [62] specific mass is represented in Fig 3.6

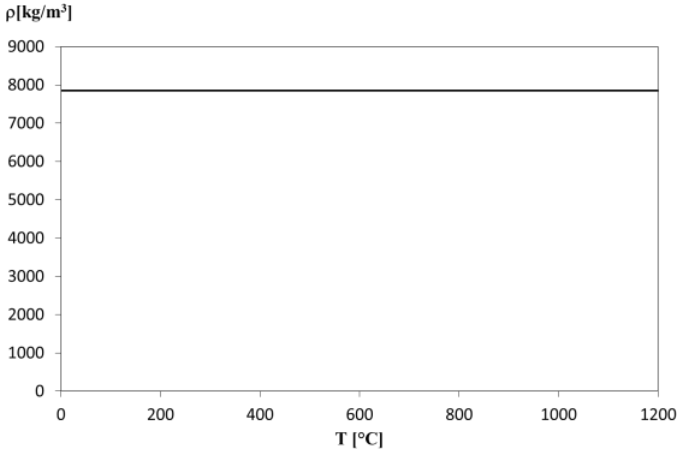

Figure 3.6: Density of concrete at elevated temperature [62]

3.3 Air

The thermal properties of air are temperature-dependent and should be used to simulate the interface between the steel deck and the bottom surface of the concrete topping. In addition, these thermal properties vary with the air pressure. This work

considers the thermal properties of air at 1 atm pressure [56].

Presently, there is no standard, which specifies the thermal properties of air. However, computer programs and experimental tests provide reliable data for numerical analyses. Figure 3.7 presents the variation of the main thermal properties of air with temperature θ_{air} (°C), namely the specific heat cair (J/kgK), the thermal conductivity λ_{air} (W/mK) and the density ρ_{air} (kg/m^3).

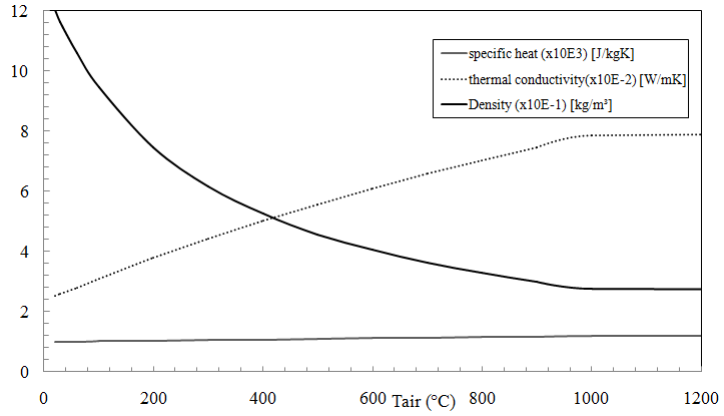

Figure 3.7: Temperature-dependent thermal properties of air at 1 atm pressure

Chapter 4

SIMPLIFIED METHOD GIVEN BY EUROCODE 4, part 1.2

Eurocode 4, part 1.2 [6] proposes different methods that allow the calculation of important parameters regarding the fire behaviour of composite slabs through simple analytical expressions slabs under standard fire ISO834 [52]. These results are generally very conservative and might be utilized for a primer design stage.

The simplified calculation methods for composite slabs with profiled steel deck are presented in the Annex D of the Eurocode 4–Part 1-2 [6].

4.1 Eurocode 4, Part 1.2

The analytical expressions for composite slabs given in the current version of the EN 1994, 1.2 are based on the study conducted by Both [1], in 1998. As stated before, no revisions were made to these methods during the last years.

The fire resistance t_i of composite slabs concerning the thermal insulation criterion is the ability to with stand fire in one side and retaining the heat flow through the slab. The temperature rise on the top surface of the slab should not exceed an average value of 140 °C or a maximum of 180°C, depends linearly on different parameters and should

be determined according to Eq 4.1.

$$t_a = a_0 + a_1 \cdot h_1 + a_2 \cdot \phi_{up} + a_4 \cdot \frac{A}{L_r} + a_4 \cdot \frac{1}{l_3} + a_5 \cdot \frac{A}{L_r} \cdot \frac{1}{l_3} \tag{4.1}$$

In the equation above, h_1 is the concrete thickness (mm); Φ_{up} is the view factor of the upper flange (eq 2.10 and 2.11) (dimensionless); A/L_r is the rib geometry factor (mm); and l_3 is the width of the upper flange (mm). The partial factors a_i are tabulated coefficients which are different for normal weight concrete (NWC) and lightweight concrete (LWC). These coefficients are given in the following table 4.1.

	a_0	a_1	a_2	a_3	a_4	a_5
	(min)	(min/mm)	(min)	(min/mm)	(mm/min)	(min)
NWC	-28.8	1.55	-12.6	0.33	-735.0	48.0
LWC	-79.2	2.18	-2.44	0.56	-542.0	52.3

Table 4.1: Coefficients for the determination of the fire resistance of composite slabs with NWC and LWC (adapted from EN 1994,1.2[6]).

The scope of this investigation comprises only composite slabs with normal weight concrete. The rib geometry factor is defined as the ratio between the concrete volume of the rib per meter of rib length A (mm^3/m) and the exposed area of the rib per meter of rib length L_r (mm^2/m). This factor can be calculated using the geometric parameters of the slab as follows.

$$\frac{A}{L_r} = \frac{h_2(\frac{l_1 + l_2}{2})}{l_2 + 2.\sqrt{h_2^2 + (\frac{l_1 + l_2}{2})}} \tag{4.2}$$

The temperatures of the parts of the steel deck θ_a (°C) should be calculated according to Eq. 4.3

$$\theta_a = b_0 + (b_1. \cdot \frac{1}{l_3}) + (b_2. \cdot \frac{A}{L_r}) + (b_3.\phi_{up}) + (b_4.\phi_{up}^2) \cdot \frac{1}{l_3} \tag{4.3}$$

In the equation above, l_3 is the width of the upper flange (mm), $\frac{A}{L_r}$ is the rib geometry factor (mm), and ϕ_{up} is the view factor of the upper flange (dimensionless). The partial

factors b_i are coefficients that differ for slabs with normal weight concrete (NWC) and lightweight concrete. Also buildings must have a fire resistance to ensure its load bearing capacity (R) for (60,90 and 120 min) , Table 4.2 presents these coefficients for each part of the steel deck for slabs with NWC.

Standard fire resistance	**Part of the steel deck**	b_0 (°C)	b_1 (°C mm)	b_2 (°C mm)	b_3 (°C mm)	b_4 (°C mm)
R60	Lower flange	951	-1197	-2.32	86.4	-150.7
	Web	661	-833	-2.96	537.7	-351.9
	Upper flange	340	-3269	-2.62	1148.4	-679.8
R90	Lower flange	1018	-839	-1.55	65.1	-108.1
	Web	816	-959	-2.21	464.9	-340.2
	Upper flange	618	-2786	-1.79	767.9	-472.0
R120	Lower flange	1063	-679	-1.13	46.7	-82.8
	Web	925	-949	-1.82	344.2	-267.4
	Upper flange	770	-2460	–1.67	592.6	-379.0

Table 4.2: Coefficients for the determination of the temperatures of the rebars in the rib for slabs with NWC for different fire ratings (adapted from EN 1994,1.2)[6]

The temperature of the rebars in the rib θ_s (°C) shall be determined according to Eq 4.4.

$$\theta_s = c_0 + (c_1.u_3/h_1) + (c_2.z) + (c_3 \cdot \frac{A}{L_r}) + (c_4.\alpha) \cdot \frac{1}{l_3} + (c_5. \cdot \frac{1}{l_3}) \tag{4.4}$$

In the equation above,u_3 is the distance of the rebar to the lower flange (mm); h_2 is the thickness of the concrete part (mm); z is an indication of the position in the rib (mm^{-05}); and a is the angle of the web (degrees). The partial factors c_i depend on the fire resistance (R) and differ for slabs with NWC and lightweight concrete. Table 4.3 gives these coefficients for slabs with NWC.[6]

Standard fire resistance	c_0 (°C)	c_1 (°C)	c_2 (°C $mm^{0.5}$)	c_3 (°C mm)	c_4 (°Cmm)	c_5 (°C mm)
$R60$	1191	-250	-240	-5.01	1.04	-925
$R90$	1342	-256	-235	-5.30	1.39	-1267
$R120$	1387	-238	-227	-4.79	1.68	-1326

Table 4.3: Coefficients for the determination of the temperatures of the rebars in the rib for slabs with NWC for different fire ratings (adapted from EN 1994,1.2)[6]

The z-factor should be calculated according to the following equation:

$$\frac{1}{z} = \frac{1}{\sqrt{u_1}} + \frac{1}{\sqrt{u_2}} + \frac{1}{\sqrt{u_3}} \tag{4.5}$$

In Eq. 4.5, u_1 and u_2 are defined as the shortest distances of the centre of the rebar to any point of the webs of the steel deck (mm); and u_3 is the distance of the centre of the rebar to the lower flange of the steel deck (mm). These parameters are illustrated in Figure 4.1.

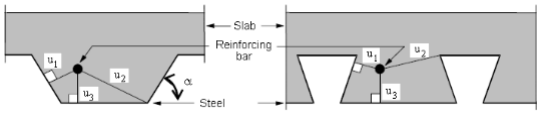

Figure 4.1: Parameters for the position of the reinforcement bars [71]

The simplified calculation method also provides general rules for the determination of the load bearing capacity of composite steel-concrete slabs. Based on a global plastic analysis, the design for bending resistance should be determined using Eq. 4.6.

$$M_{fi,t,Rd} = \sum_{i=1}^{n=4} A_i \cdot z_i k_{y,\theta,i} \cdot (\frac{f_{y,i}}{\gamma_{M,fi}}) + \gamma_{slab} \cdot \sum_{j=1}^{m=1} A_j \cdot z_j \cdot k_{c,\theta,j} \cdot (\frac{f_{c,j}}{\gamma_{M,fi,c}}) \tag{4.6}$$

The coordinates z_i and z_j are the distances of the components for steel and concrete materials, between the geometric centre and the neutral axis of the slab under fire conditions. The coefficients $k_{y,\theta,i}$ and $k_{c,\theta,i}$ represent the reduction coefficients for the

yielding stress of steel and the compressive strength of concrete, affected by the temperature of each component, being defined by standards for steel [62] and concrete [61]. The coefficient $k_{y,\theta,i}$ may have different values. Reduction factors for elevated temperatures, $k_{y,\theta,i}$, for the steel sheet, the reduction factors $k_{y,\theta,i}$ are given in EN1993-1-2.For the reinforcement the reduction factor is given in EN1994-1-2 , because the reinforcement bars are cold worked. According to the type of steel (cold-formed carbon steel for the design of class 4 sections at elevated temperatures [6] and cold-formed carbon steel for rebars [61]). The model assumes no reduction for concrete.

Chapter 5

NUMERICAL SOLUTION METHOD

5.1 ANSYS Software

ANSYS is a general-purpose finite element package for numerically solving a wide variety of physical problems. These problems include static/dynamic structural analysis (both linear and non-linear), heat transfer and fluid problems, as well as acoustic and electro-magnetic problems.

With ANSYS, it is possible to analyse models from the simplest to the most complex, with extreme flexibility and with the advantage of being a software already used by the scientific community and the industry. The domain is subdivided into small discrete regions, known as finite elements. These elements are defined by geometry, and mathematic entities, nodes: This method is based on interpolation functions and numerical integration methods [67].

The ANSYS PLANE 55 element was used for the analysis of thermal effects on the analysed structures, which has thermal conduction capacity in two dimensions, 2D. The element has four nodes and a single degree of freedom at each node, the temperature. [67].The element is shown in figure 5.1 (ANSYS library)

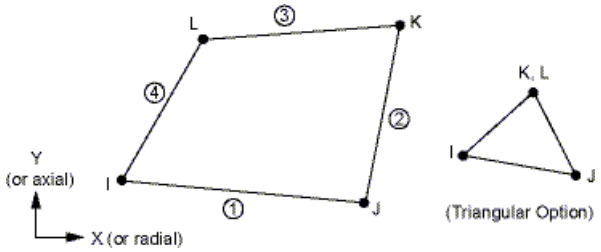

Figure 5.1: Geometry of the PLANE 55 element (ANSYS library)

5.2 Finite element models for thermal analysis

In ANSYS, the three-dimensional geometric models of the composite slab are manually created using the graphical user interface, by definition of key points, lines, areas and volumes (through the extrusion of areas). Figure 5.2 presents the geometric model of a composite slab introduced in the software.

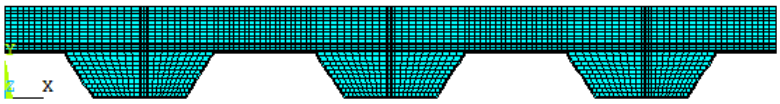

Figure 5.2: Modelling of composite slabs in ANSYS areas and volumes

The thermal properties, are introduced on the software by creating material models for each material; that is, manually inserting the values of each property for different instants of time. These material models can be written to a MP file to be read in posterior simulations.

A specific number of divisions are given for each line in order to generate the mesh. The finite element model is created by meshing areas using-the same 2-D finite elements, appropriate for thermal analysis, for each subdomain (steel components, concrete topping, and the air gap).

Elements used in numerical models

Different types of elements are going to be applied to solve the thermal and the mechanical analysis. These elements are defined in the data base of the software ANSYS. The elements were selected according to the simulation needs, using the lower-order finite elements available.

5.3 Initial boundary conditions

An initial uniform temperature is applied to all the meshed nodes (20ºC). The lower part of the deck is submitted to standard fire conditions, using a convection coefficient of 25 $[W/m^2K]$ and an emissivity of the fire equal to 1. These parameters are depicted in the Figure 5.3. The upper part of the slab is submitted to a convective coefficient of 9 $[W/m^2K]$ to include the radiation effect [68].

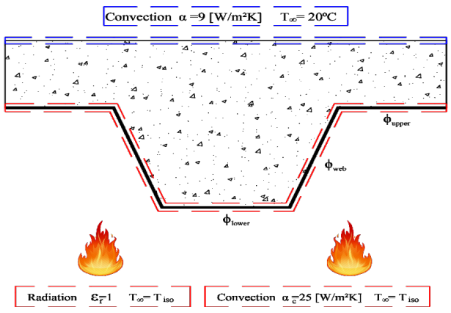

Figure 5.3: Boundary conditions for the slab with trapezoidal steel deck [70]

5.4 Validation of the numerical result

The validation of the numerical result (ANSYS) with the experimental results was made using an air gap [69]. For the slab under analysis, the air gap was considered to be 0.5 mm. Figure 5.4, depicts the model, and Figure 5.5 represents the temperature development (numerical and experimental) at different selected points temperatures (temperature

locations ($T17$, $T19$, $T20$) there is a difference between the two results especially in the point ($T20$) (lower flange) and ($T17$) (upper flange) because these points are in direct contact with the fire.

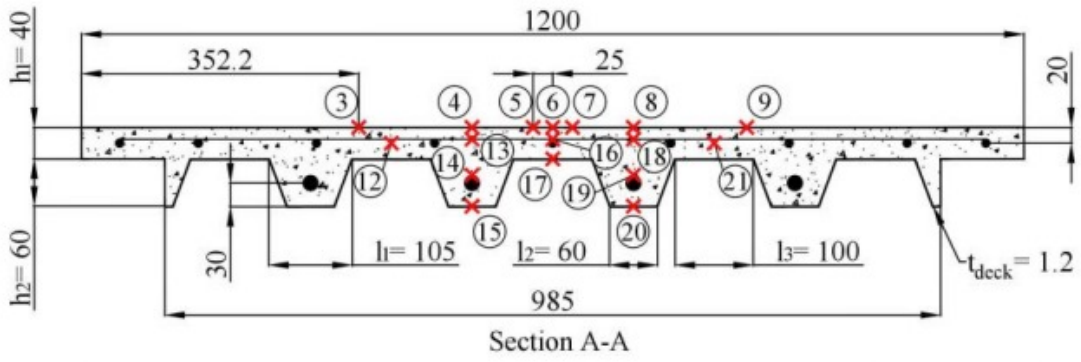

Figure 5.4: Comparison between the experimental and Numerical results with t_a = 0.5 mm [2]

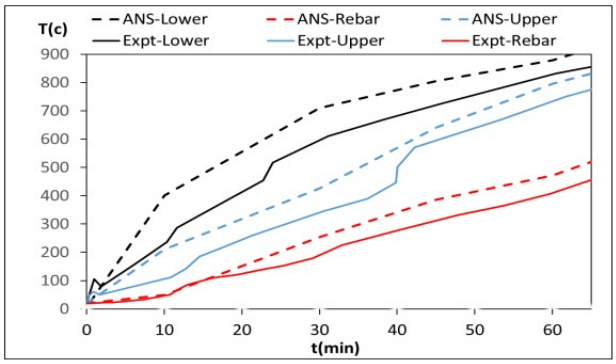

Figure 5.5: Profile of the composite slab with different points

Figure 5.5, compare the experimental results obtained by Lucas M.S Prates [2] with the numerical values obtained with air gap (t_a equal to 0.5 mm). Based on the results obtained with values of t_a , we observed that the results is close to the experimental. Therefore, the next simulations are done using t_a = 0.5 mm.

Chapter 6

PARAMETRIC ANALYSIS

6.1 Description

A parametric study comprising four commercial steel deck profiles with different concrete heights h1 and different slabs geometries was carried out in this investigation.A representative portion of 1 m by 1 m of each slab is selected for performing thermal analyzes taking into account standard fire conditions. In addition, a moisture content of 3% of the weight of the concrete is considered. All composite slabs are exposed to fire for 7200 seconds (2 hours). In this parametric study, the focus is on the influence of the various parameters on the temperatures of the parts of the composite slab, namely the thickness of slabs. In total, 16 numerical simulations were carried out in ANSYS using an air gap of 0.5 mm. The Table 6.1 summarizes the ranges of the parameters studied, where td is the steel deck thickness.

Steel deck profile	**h1 (mm)**	**td (mm)**
Cofraplus60 (Trapezoidal))	50, 70, 90,1105	1.25
Polydeck 59S (Trapezoidal)	50, 70, 90,110	1.25
Multideck (Re-entrant)	50, 70, 90,110	1.2
Bondek (Re-entrant)	50, 70, 90,110	1.2

Table 6.1: Investigated parameters of the first parametric study

The ranges of selected parameters comprise commonly used values. The diameters and spacing of the anti-crack meshes have been determined from technical catalogs. Figure 6.1 illustrates the geometry of the steel deck profiles, corresponding to current models available on the market.

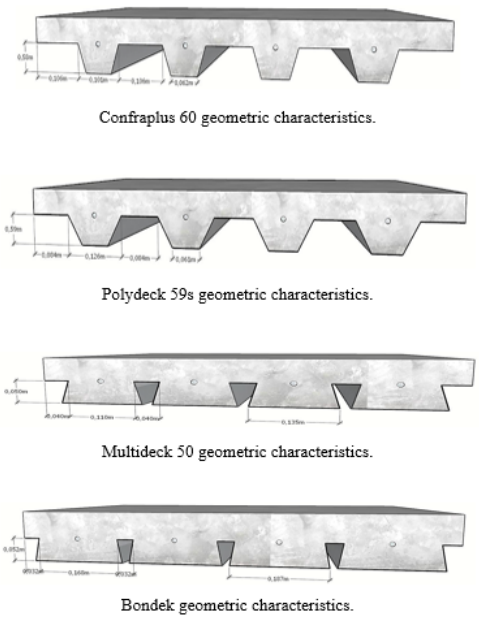

Figure 6.1: Steel deck geometries for the first parametric study (dimensions in millimeters) (adapted from [70]).

The parametric study also examined the effect of concrete thickness (h_1) and air gap (t_a) on fire resistance according to the insulation standard, and 24 numerical simulations were performed in ANSYS, using the model of the air gap with 0.5 mm.

6.1.1 Steel deck geometry

Comparing the results of different geometry steel decks for simulations with the same concrete thickness, the slabs with re-entrant profiles present higher bending moment resistance in comparison to the slabs with trapezoidal profiles. This is explained by the fact that the re-entrant profiles allow the employment of a more uniform volume of

concrete along the cross-section,resulting in more homogeneous temperature distributions. Figure 6.2 illustrates the influence of the geometry steel deck on sagging moment of each slab for different fire ratings,assuming $h_1 = 50$.

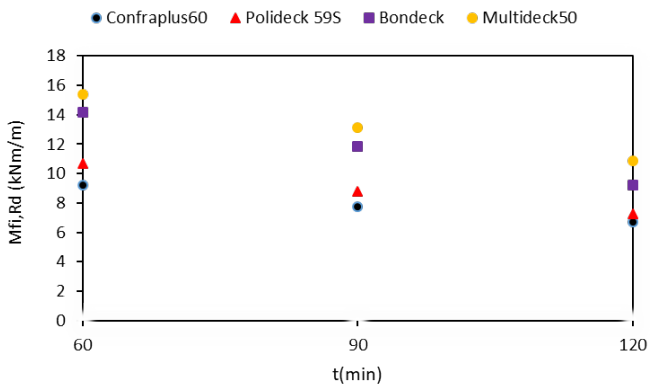

Figure 6.2: Different geometry steel deck on sagging moment of each slab of the first parametric study

6.1.2 Concrete thickness

The thickness of the slab (the thickness of the concrete was modified (h_1), assuming 4 different thicknesses of concrete (h_1= 50 mm, h_1= 70 mm, h_1= 90 mm, h_1= 110 mm) were tested trapezoidal (Confraplus50) and re-entrant (Bondeck), and it was noted that the change in the thickness of the concrete has not effect in the temperature of the components (Lower, Upper flange and Web) because these parts are located at the bottom of the slab and are related to steel more than the thickness of the concrete. Almost the same results were obtained, for rebar, where there is small change in temperature, with the increase in the thickness of concrete, the temperature decreases.

By comparing the results of simulation operations with different thicknesses, a slight difference in temperature was observed for each of the thicknesses $(50, 70, 90, 110)$ with trapezoidal and re-entrant, however, when the concrete increased in height, the temperature decreased, even if relatively.

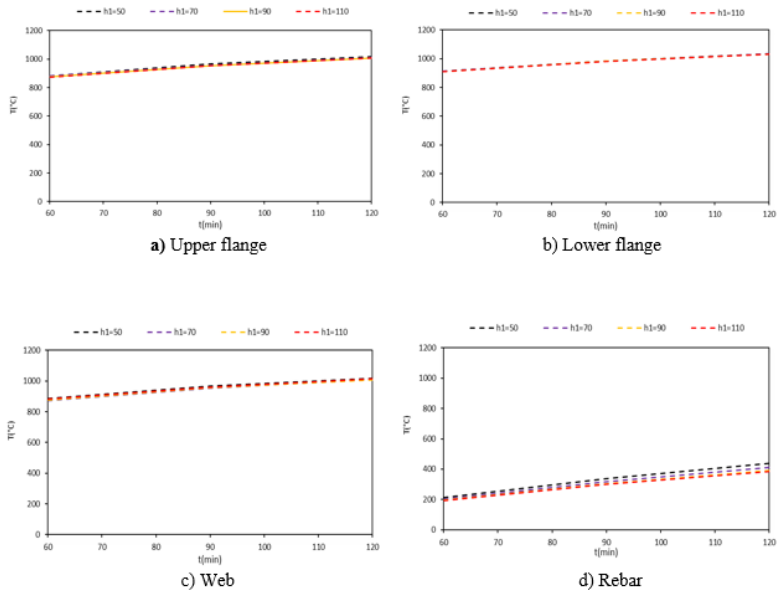

Figure 6.3: Influence of concrete thickness on (Lower, Upper and Web, Rebar) of the slabs Confraplus50

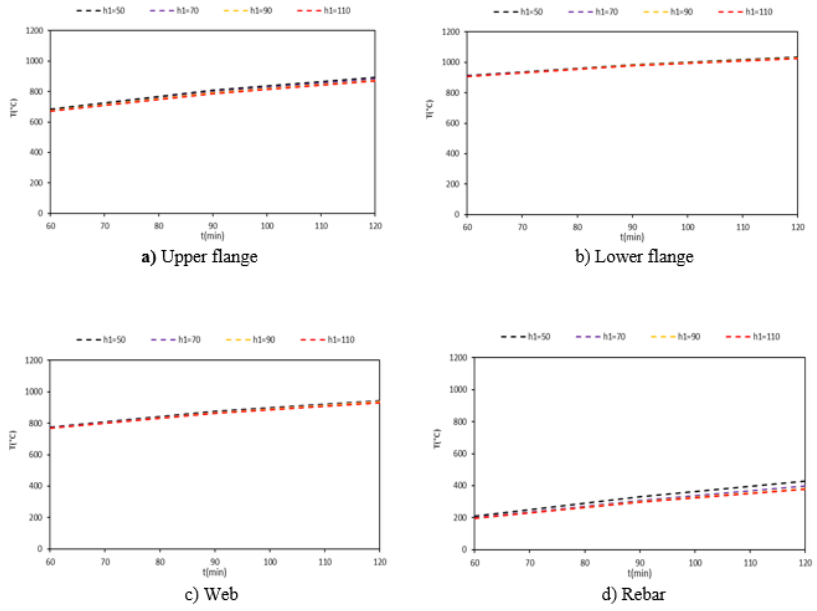

Figure 6.4: Influence of concrete thickness on (Lower, Upper and Web, Rebar) of the slabs Bondeck

6.2 Numerical results and Eurocode 4, Part 1.2

Figure 6.5 present the comparison between numerical results and results obtained with the simplified calculation method of Eurocode 4, Part 1.2 (EC4) for on sagging moment $M_{fi,Rd,sag}$ depending on the effective thickness of the composite slabs using four types of steel deck.

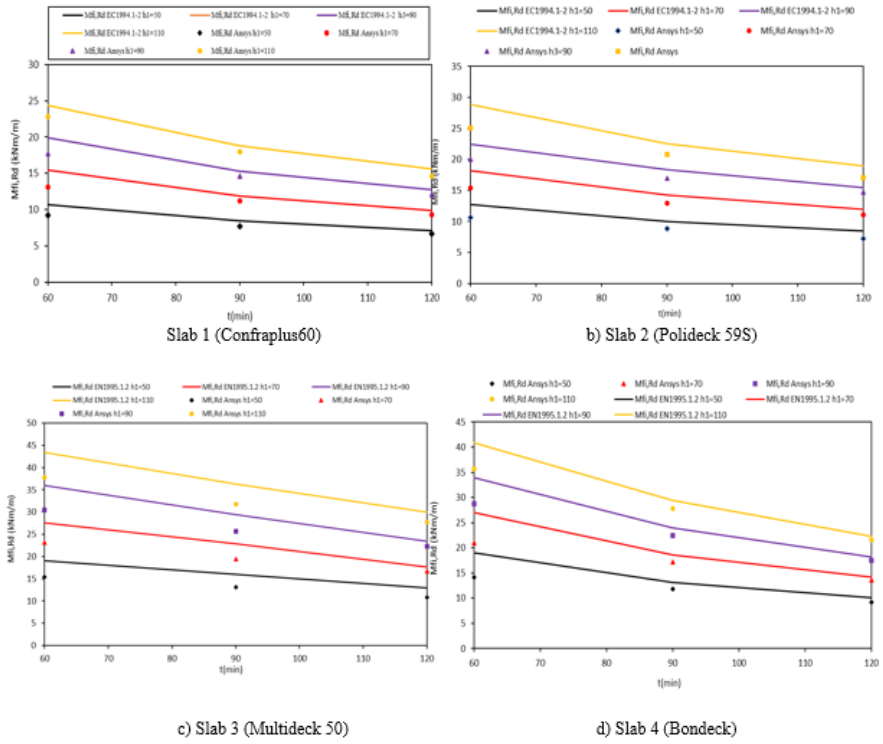

Figure 6.5: Comparison between the numerical results from ANSYS and Eurocode 4, Part 1.2 sagging moment.

In general, it is observed that the results from the Eurocode 4, Part 1.2 for the sagging moment are considerably higher to the numerical results. Therefore, when the concrete height of the slab increases, the sagging moment increases.

7. CONCLUSION

This work deals with 2-D numerical simulations of the fire behaviour of composite slabs with profiled steel deck using the software ANSYS Mechanical APDL. In this regard, numerical models have been established considering an insulating layer (air gap) with constant thickness between the concrete topping and the steel deck to simulate debonding effects. A study has been performed using different composite slabs, in order to evaluate the influence of different parameters on the temperature of the steel components, and on sagging moment. The developed numerical models satisfactorily predicted the fire behaviour of composite slabs by describing the two-dimensional heat flow through this structural element in good agreement with experimental results. Temperature of the steel components obtained through the calculation rules from EN 1994, part 1.2 were on the unsafe side for most of the cases.

This research presents the fire behaviour of structures is of great importance and complexity in the field of civil and construction engineering. Additional research shall be carried out in the future in order to complement the results of this work:

a) Influence of the thickness of the concrete of the ISO834 fire resistance of composite slabs.

b) Conduct experimental fire tests with composite slabs with trapezoidal and re-entrant steel deck profile.

8. REFERENCES

[1] Fernando Freire Ribeiro"numerical simulation of composite slabs with steel deck under fire conditions"Polytechnic Institute of Bragança – IPB, july ,2019

[2] Prates, L.M.S.: Numerical simulation of the fire behaviour of composite strucures (slabs) [in Portuguese]. Master's Thesis, Politechnic Institute of Bragança (2018)

[3] L.Calado and J.Santos, Steel-concrete composite structures [in portuguese].Lisbon: IST press, 2010.

[4] Abdel-Halim, M.A.H., Hakmi, M.R., O'Leary, D.C.: Fire resistance of composite floor slabs using a model fire test facility. Eng. Struct. 21, 176–182 (1999)

[5] J. M. Davies and H. B. Wang, "Numerical temperature calculation for composite deck slabs exposed to fire," Trans. Eng. Sci., vol. 5, pp. 331–338, 1994.

[6] CEN - European Committee for Standardization, EN 1994-1-2: Design of composite steel and concrete structures - Part 1-2: General rules - Structural fire design. Brussels, 2005.58

[7] C. Both, J. H. H. Fellinger, and L. Twilt, "Shallow floor construction with deep composite deck: from fire tests to simple calculation rules," Heron, vol. 42, no. 3, pp.

[8] D. L. Logan, A first course in the Finite Element Method, 4th ed. Platteville: Thomson, 2007.

[9] G. M. E. Cooke, R. M. Lawson, and G. M. Newman, "Fire resistance of composite deck slabs," Struct. Eng., vol. 66, no. 16, pp. 253–267, 1988.

[10] D. A.Nethercot, Composite Construction. London: Spon Press, 2004.

[11] J. Jiang, J. A. Main, J. M. Weigand, and F. H. Sadek, "Thermal performance of composite slabs with profiled steel decking exposed to fire effects," Fire Saf. J., vol. 95, no. May 2017, pp. 25–41, 2018.

[12] A. Penza, "Composite Slabs with Lightweight Concrete: Experimental evaluation

[13] B. F. Friberg, “Combined Form and Reinforcement to Concrete Slabs,” J. Am. Concr. Inst., vol. 50, no. 5, pp. 697–716, 1954.

[14] O. Pettersson, S. E. Magnusson, and J. Thor, “Fire engineering design of steel structures,” Lund, 1976.

[15] R. Hamerlinck, “The behaviour of fire-exposed composite steel/concrete slabs,” Eindhoven University of Technology, 1991.

[16] European Convention for Constructional Steelwork - Committee T3 - Fire Safety of Steel Structures, “Calculation of the fire resistance of composite concrete slabs with profiled steel sheet exposed to the standard fire,” Brussels, 1983.

[17] International Standard ISO 834, “Fire-resistance tests - Elements of building construction.” 1975.

[18] H. D. Wright, H. R. Evans and P. W. Harding “The Use of Profiled Steel Sheeting in Floor Construction”, Journal of Constructional Steel Research, 7 (1987) 279-295.

[19] W.Samuel Easterling, Craig S.Young, Associate Members, ASCE “Strength of composite slabs”,Journal of Structural Engineering, 1992.118:2370-2389.

[20] Pentti Makelainen, Ye Sun “The longitudinal shear behaviour of a new steel sheeting profile for composite floor slabs”Journal of Constructional Steel Research, 49 (1999) 117–128.

[21] Matthew J. Burnet, Deric J. Oehlers, “Rib shear connectors in composite profiled slabs”,Journal of Constructional Steel Research 57 (2001) 1267–1287.

[22] S. Chen, “Load carrying capacity of composite slabs with various end constraints”Journal of Constructional Steel Research, 59 (2003) 385–403

[23] Miquel Ferrer, Frederic Marimon, Michel Crisinel “Designing cold-formed steel sheets for composite slabs: An experimentally validated FEM approach to slip failure mechanics”,Thin-Walled Structures,44 (2006) 1261–1271.

[24] G. Marciukaitis, B .Jonaitis, J. Valivonis, “Analysis of deflections of composite slabs with profiled sheeting up to the ultimate moment” Journal of Constructional Steel Research,62 (2006) 820–830.

[25] V.Marimuthu S. Seetharaman, S. Arul Jayachandran, A. Chellappan, T.K. Bandyopadhyay, D. Dutta "Experimental studies on composite deck slabs to determine the shear-bond characteristic (m –k) values of the embossed profiled sheet", Journal of Constructional Steel Research, 63 (2007) 791–803.

[26] Youn-JuJeong, "Simplified model to predict partial interactive structural performance of steel concrete composite slabs", Journal of Constructional Steel Research, 64 (2008) 238–246.

[27] Melchor López, Ávila,Rafael, Larrúa Quevedo, Carlos A. Recarey Morfa, "Evaluating longitudinal shear resistance in composite slabs with steel decks",RevistaIngeniería de Construcción,Vol. 24 No 1, Abril de 2009.

[28] Redzuan Abdullah, W. Samuel Easterling, "New evaluation and modeling procedure for horizontal shear bond in composite slabs","Journal of Constructional Steel Research",65 (2009) 891–899.

[29] NoémiSeres-László Dunai, "Experimental investigation of an individual embossment for composite floor design", Concrete structures (2011).

[30] Baskar. R, "Experimental and Numerical Studies on Composite Deck Slabs",International Journal of Engineering and Technology, July, 2012

[31] J. Holomeka, M. Bajera, "Experimental and Numerical Investigation of Composite Action of Steel Concrete Slab", Procedia Engineering, 2012

[32] Namdeo Adkuji Hedaoo1, Laxmikant Madanmanohar Gupta2 and Girish Narayanrao Ronghe2, "Design of composite slabs with profiled steel decking: a comparison between experimental and analytical studies" International journal of advanced scientific engineering, 2012

[33] K.N. Lakshmikandhan P .Sivakumar,R .RavichandranandS. Arul Jayachandran

"Investigations on Efficiently Interfaced Steel Concrete Composite Deck Slabs", Journal of Structures,Volume 2013, Article ID 628759.

[34] Héctor Cifuentes, "Fernando Medina, "Experimental study on shear bond behavior of composite slabs according to Eurocode 4"Journal of Constructional Steel Research,82 (2013) 99–110.

[35] R.P. Johnson, A.J. Shepherd, “Resistance to longitudinal shear of composite slabs with longitudinal reinforcement”, Journal of Constructional Steel Research, 82 (2013) 190–194

[36] A. Gholamhoseini, R.I. Gilbert, M.A. Bradford, Z.T. Chang, “Longitudinal shear stress and bond–slip relationships in composite concrete.

[37] Japan U. Shah, Prof. Merool D. Vakil“Parametric study of Composite Slab Using Finite Element Analysis”, International Journal of Futuristic Trends in Engineering and Technology ISSN: 2348-5264 (Print), ISSN: 2348-4071 (Online) Vol. 1 (03), 2014.

[38] Jiang, J., Main, J.A., Sadek, F.H., Weigand, J.M.: Numerical modeling and analysis of heat transfer in composite slabs with profiled steel decking. Tech. Rep. (2017)

[39] ABNT: NBR 14323 - structural fire design of steel and composite steel and concrete structures for buildings [in Portuguese] (2013

[40] Li, G.Q., Zhang, N., Jiang, J.: Experimental investigation on thermal and mechanical behaviour of composite floors exposed to standard fire. Fire Saf. J. 89, 63–76 (2017)

[41] Lim, L., Wade, C.: Experimental fire tests of two-way concrete slabs—fire engineering research report 02/12. Tech. Rep., University of Canterbury (2002

[42] J. Jiang, A. Pintar, J. M. Weigand, J. A. Main, and F. Sadek, “Improved calculation method for insulation-based fire resistance of composite slabs,” Fire Saf. J., 2019.117

[43] P. A. G. Piloto, C. Balsa, F. Ribeiro, L. Santos, R. Rigobello, and E. Kimura, “Critical temperature for the components of composite slabs with steel deck under fire for load-bearing rating,” in 4th International Conference on Numerical and Symbolic Computation Developments and Applications - SYMCOMP 2019, 2019, no. ISBN 978-989-99410-5-2, pp. 119–135.

[44] P. A. G. Piloto, C. Balsa, F. Ribeiro, L. Santos, R. Rigobello, and E. Kimura, “Fire resistance of composite slabs with steel deck: experimental and numerical investigation,” MATTER Int. J. Sci. Technol., no. ISSN 2454-5880, 2019.

[45] P. Piloto, C. Balsa, F. Ribeiro, R. Rigobello, L. Santos, and E. Kimura, “Validation models on the fire resistance of composite slab with steel deck,” in Congress on Numerical Methods in Engineering – CMN 2019, 2019, no. ISBN: 978-989-54496-0-6, pp. 625–642.

[46] C. Balsa, F. F. Ribeiro, P. A. G. Piloto, and R. Rigobello, “Numerical simulation of composite slabs with steel deck under fire conditions,” in 5th Iberian-Latin American Congress on Fire Safety - V CILASCI, 2019.

[47] P. A. G. Piloto, C. Balsa, F. F. Ribeiro, and R. Rigobello, “Improved calculation methods for the temperature of the steel components of composite slabs under fire conditions,” in Conference on Steel and Composite Construction - XII CMM,

[48] del Coz-Díaz, Juan José, et al. "Comparative study of LightWeight and Normal Concrete composite slabs behaviour under fire conditions." Engineering Structures 207 (2020): 110196.

[49] Piloto, Paulo AG, et al. "Effect of the load level on the resistance of composite slabs with steel decking under fire conditions." *Journal of Fire Sciences* 38.2 (2020): 212-231.

[50] Bolina, Fabricio, Bernardo Tutikian, and João Paulo C. Rodrigues. "Thermal analysis of steel decking concrete slabs in case of fire." *Fire Safety Journa* 121 (2021): 103295.

[51] Ministry of Internal Affairs, Decree No. 1532/2008, Technical regulation of fire safety in buildings (in Portuguese), December 29, 2008.

[52 ISO 834-1. “Fire-resistance tests - Elements of building construction – Part 1: general requirements”. 1999.

[53] Law, M. "Designing fire safety for steel–recent work." Proceedings of the ASCE Spring Convention, American Society of Civil Engineers. 1981. A. H. Buchanan and A. K. Abu, Structural design for fire safety, Second Ed. Chichester, UK: John Wiley & Sons Ltd, 2017.

[54] R. Regobello, “Numerical analysis of steel and composite steel-concrete cross sections and structural elements in fire situation [in portuguese],” University of São Paulo, 2007.

[55] Y. A. Çengel and A. J. Ghajar, Heat and mass transfer: fundamentals & applications, Fifth edit. New York: McGraw-Hill Education, 2015.118

[56] CEN - European Committee for Standardization, EN 1991-1-2: Actions on structures - Part 1-2: General actions - Actions on structures exposed to fire.Brussels, 2002.

[58] P. A. G. Piloto, “Experimental and numerical analisys of metalic structures behaviour under fire conditions [in portuguese],” University of Porto, 2000.

[59] J. P. Holman, Heat transfer, Tenth edit. New York: McGraw-Hill Education, 2010.

[60] Y. Wang, Steel and composite structures: behaviour and design for fire safety, vol. 1. London: Spon Press, 2002.

[61] CEN - European Committee for Standardization, EN 1992-1-2: Design of concrete structures - Part 1-2: General rules - Structural fire design. Brussels, 2004.

[62] CEN - European Committee for Standardization, EN 1993-1-2: Design of steel structures - Part 1-2: General rules - Structural fire design. Brussels, 2005.

[63] C.Both (1998), “The Fire Resistance of Composite Steel-Concrete Slabs”, Ph.D. thesis, Delft University of Technology.

[64] L. Lim, Andrew Buchanan, Peter Moss, Jean Marc Franssen, “Numerical Modelling of Two Way Reinforced Slabs in Fire”, Engineering Structures 26 (2004), Pg. 1081-1091.

[65] C. G. Bailey, S. Guo (2011), “Experimental behaviour of composite slabs during heating and cooling phases of fire”, Engineering Structures 33, Pg. 563-571.

[66] S. Guo (PRATE2012), Experimental and numerical study on restrained composite slab during heating and cooling, Journal of Constructional Steel Research 69, Pg.95-105

[67] Coelho, Nailde de Amorim, João Henrique da Silva Rêgo, and Lineu José Pedroso. "COMPARAÇÃO DE RESULTADOS ANALÍTICOS PARA A EQUAÇÃO DO CALOR COM O ANSYS."

[68] Piloto, P. A. G., et al. "Fire resistance of composite slabs withp rofiled steel decking: trapezoidal and reentrant numerical simulation." 6as Jornadas de Segurança aos Incêndios Urbanos e das 1as Jornadas de Proteção Civil (2018): 169-177.

[69] S. Lamont, A. S. Usmani, and D. D. Drysdale, “Heat transfer analysis of the composite slab in the Cardington frame fire tests,” Fire Saf. J., vol. 36, no. 8, pp. 815–839, 2001.

[70] [70] Silveira, Matheus Bez da. New developments on the bending resistance in composite slabs with steel deck under fire. Diss. 2022.

[71] dos Santos, Cristina Calmeiro, and João Paulo Correia Rodrigues. "7as Jornadas de Segurança aos Incêndios Urbanos 2as Jornadas de Proteção Civil."

ANNEX A

TECHNICAL FILES FOR THE FIRST PARAMETRIC ANALYSES

Steel deck: Trapezoidal – Confraplus60

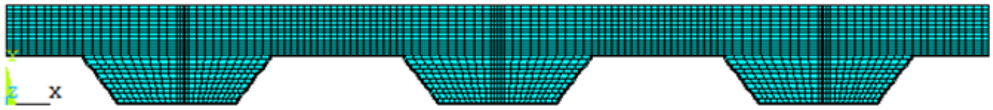

Finite element mesh- h_1= 50 mm

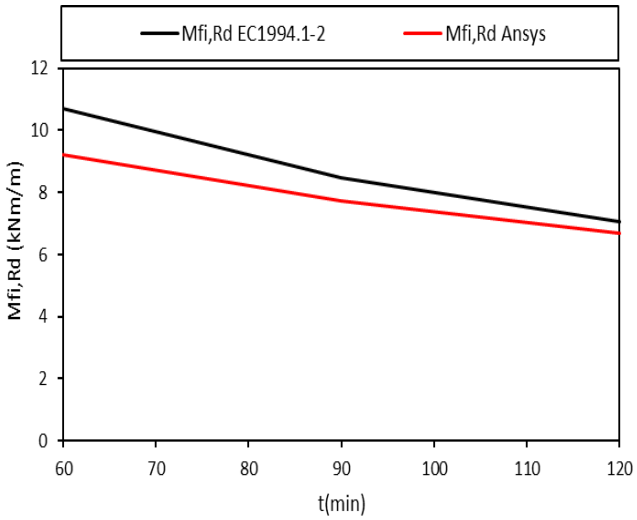

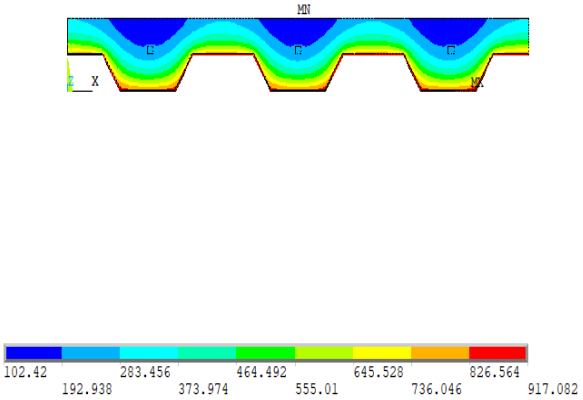

Slab1:h_1=50mm t=60 min

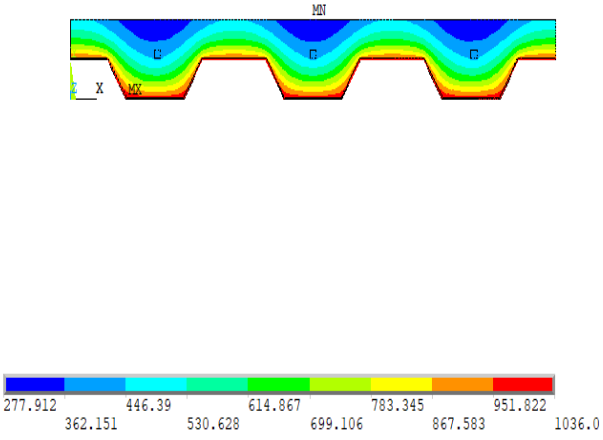

Slab3:h_1=50mm t=120 min

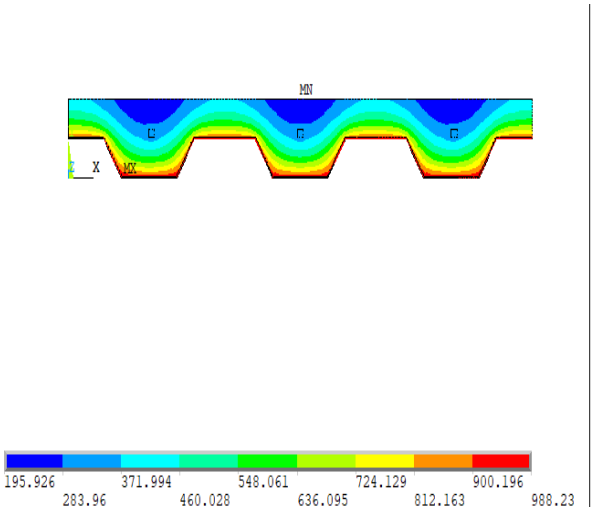

Slab2:h_1=50mm t=90 min

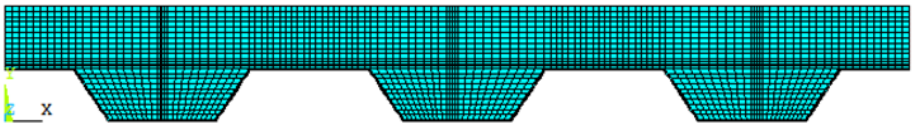

Finite element mesh-h_1=70 mm

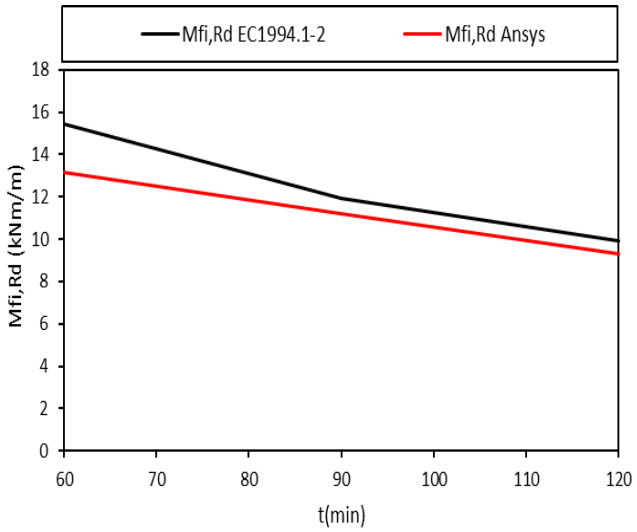

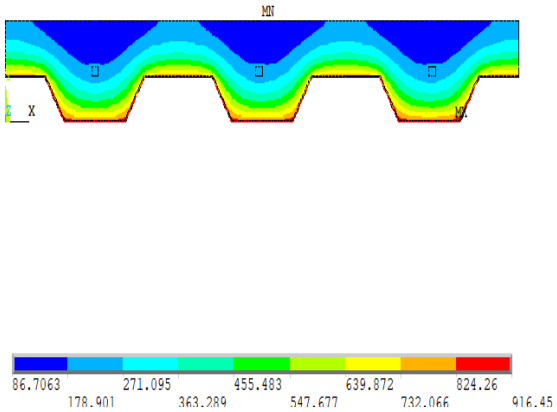

Slab4:h_1=70mm t=60 min

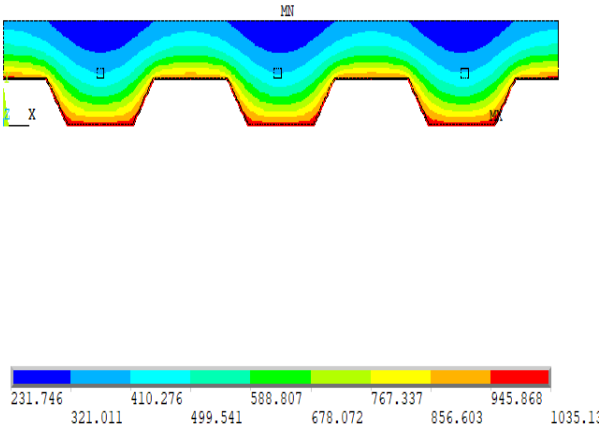

Slab6:h_1=70mm t=120 min

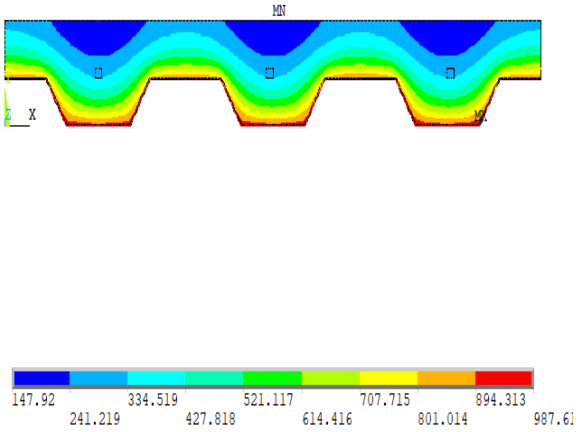

Slab5:h_1=70mm t=90 min

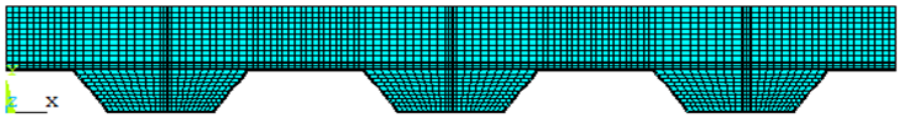

Finite element mesh- h_1= 90 mm

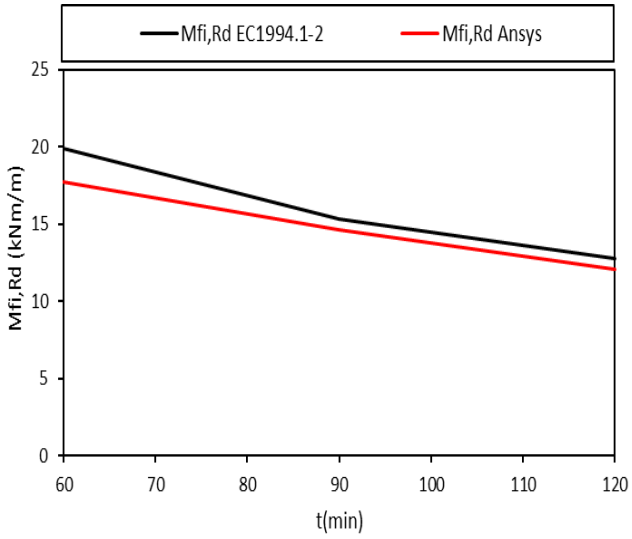

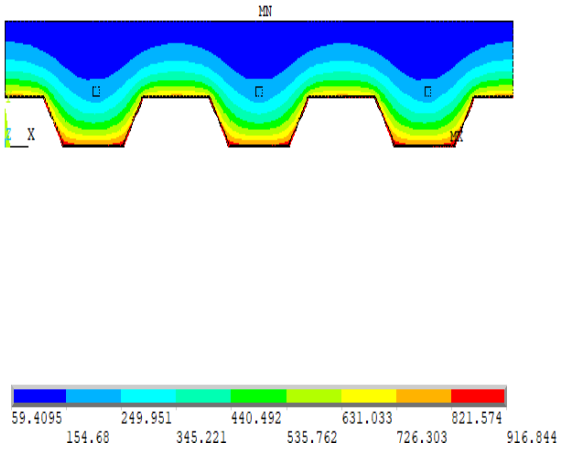

Slab7:h_1=90mm t=60 min

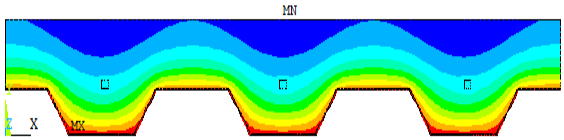

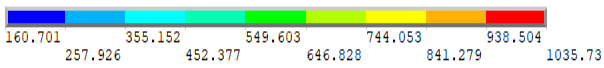

Slab9:h_1=90mm t=120 min

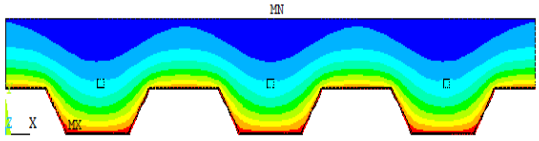

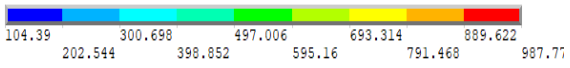

Slab8:h_1=90mm t=90 min

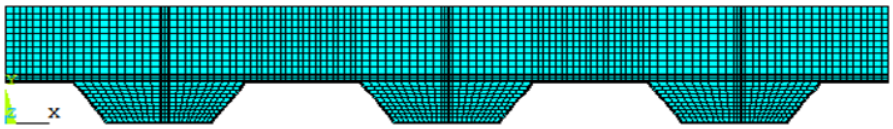

Finite element mesh- h_1= 110 mm

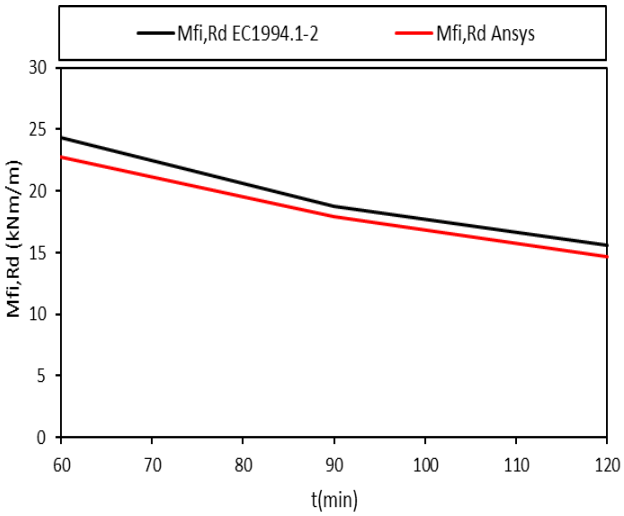

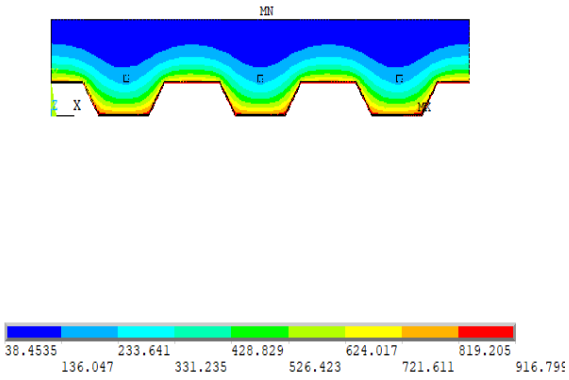

Slab10: h_1=110mm t=60 min

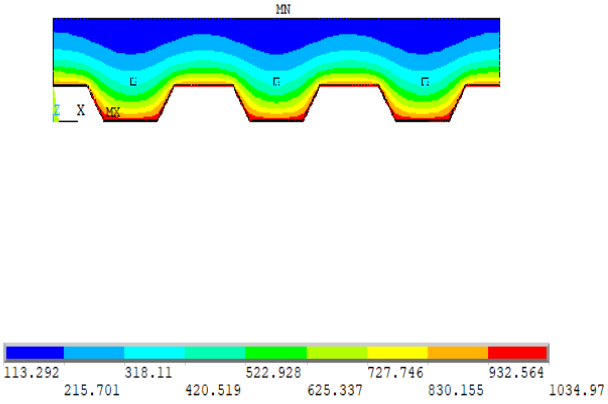

Slab12: h_1=110mm t=120 min

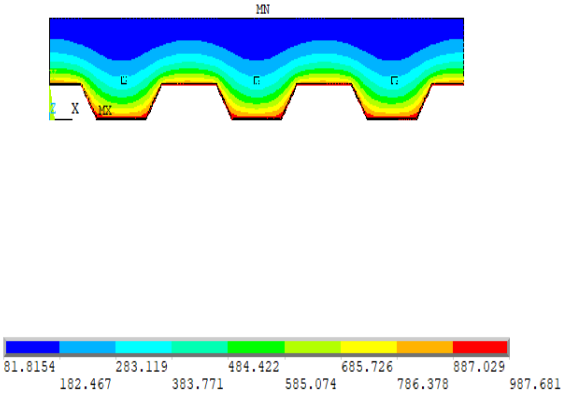

Slab11: h_1=110mm t=90 min

Steel deck: Reentrant – Bondeck

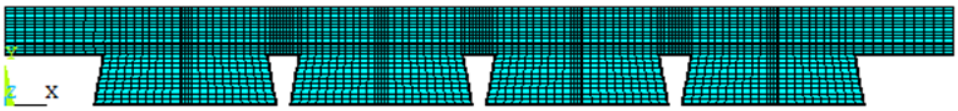

Finite element mesh- h_1= 50 mm

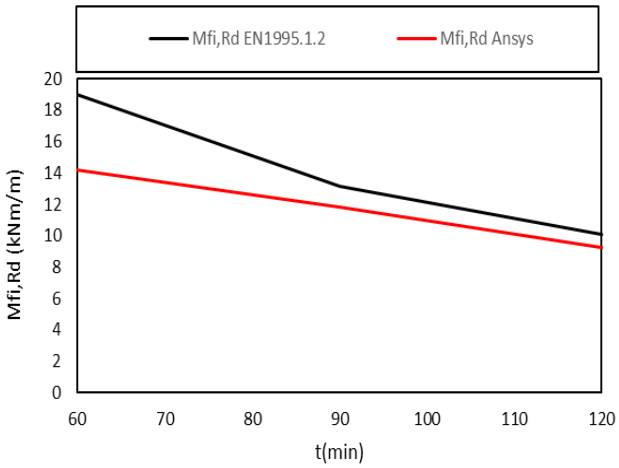

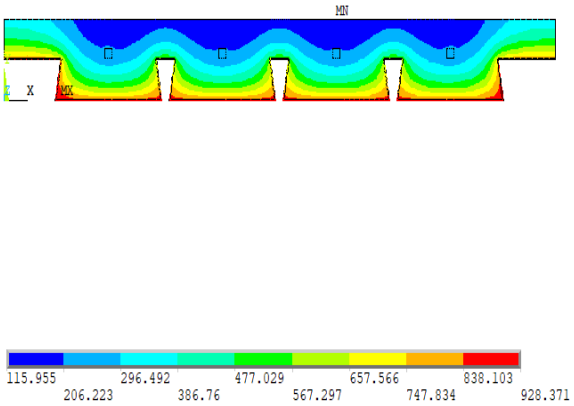

Slab13: h_1=50mm t=60 min

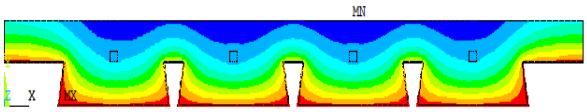

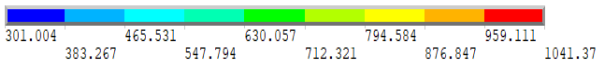

Slab15: h_1=50mm t=120 min

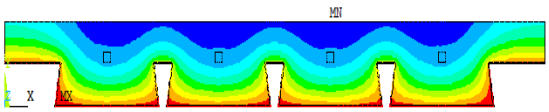

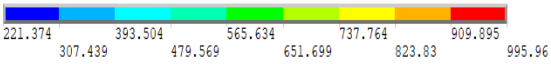

Slab14: h_1=50mm t=90 min

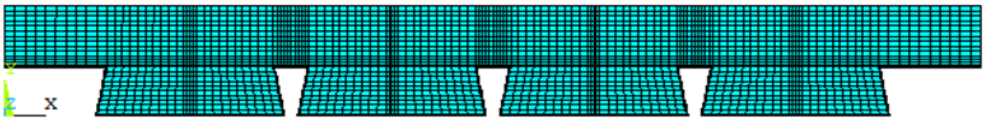

Finite element mesh- h_1= 70 mm

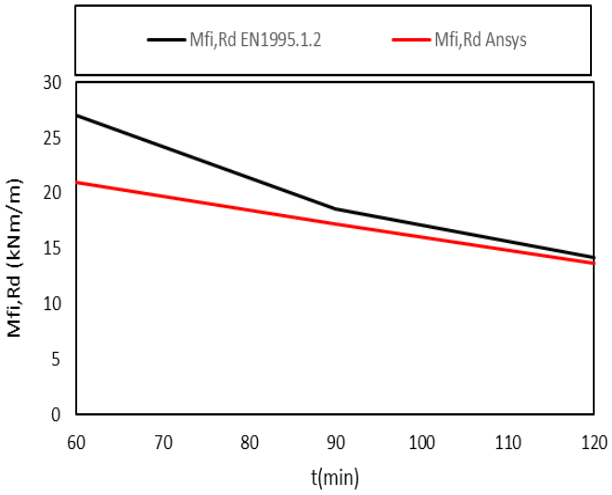

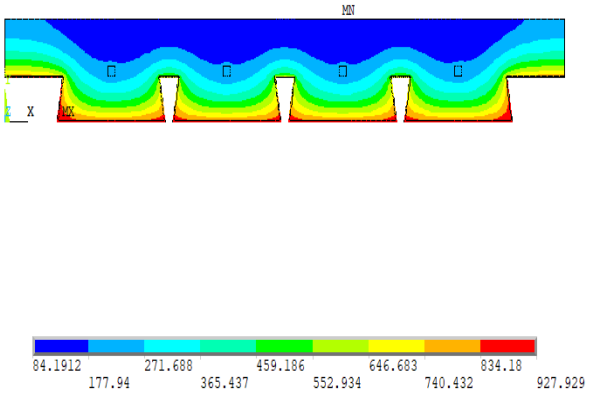

Slab16:h_1=70mm t=60 min

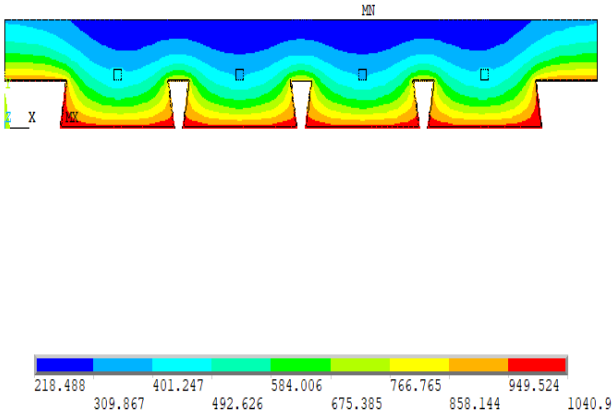

Slab18: h_1=70mm t=120 min

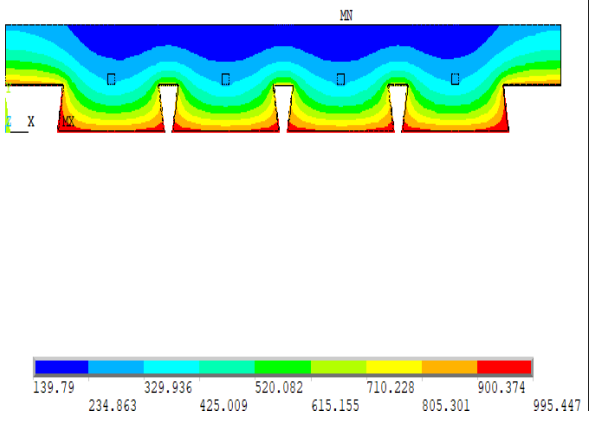

Slab17: h_1=70mm t=90 min

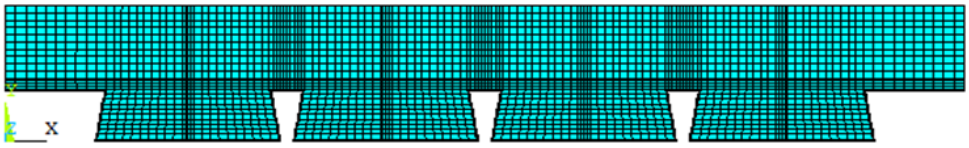

Finite element mesh- h_1= 90 mm

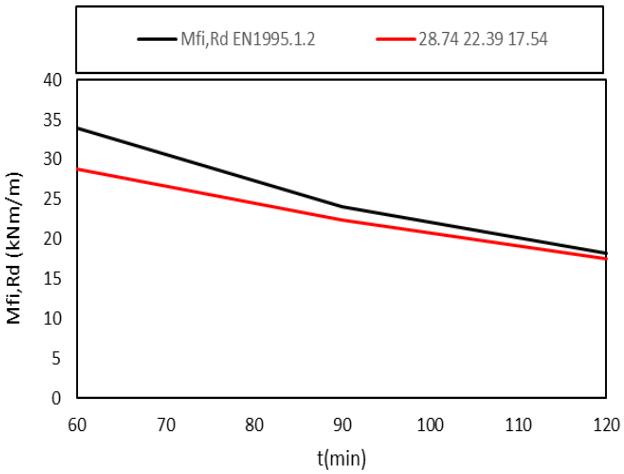

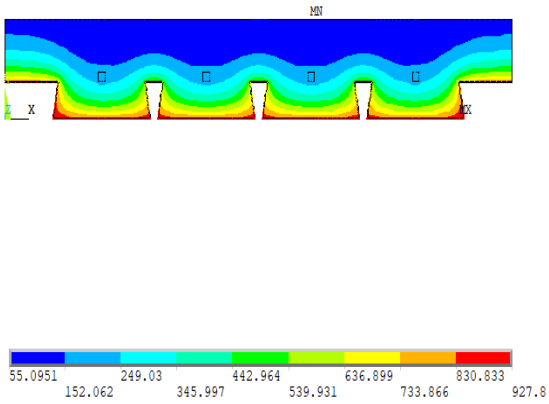

Slab19: h_1=90mm t=60 min

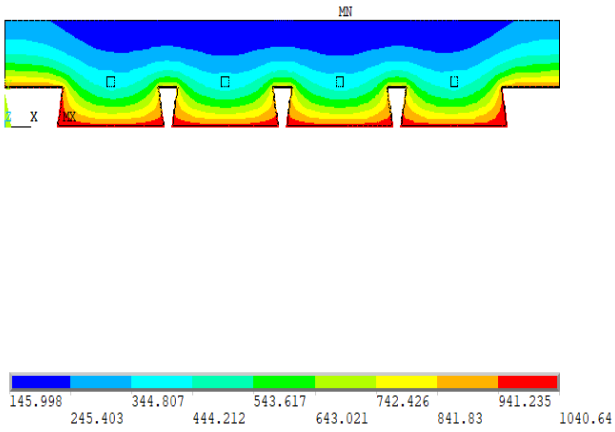

Slab21: h_1=90mm t=120 min

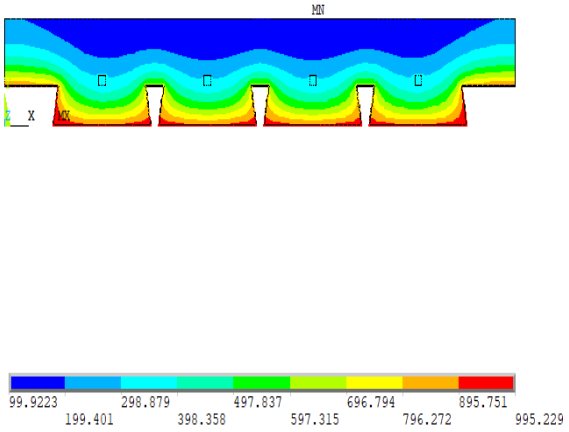

Slab20: h_1=90mm t=90 min

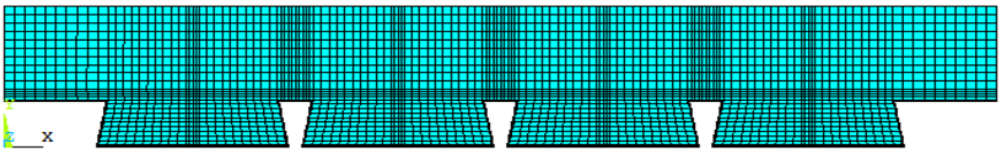

Finite element mesh- h_1= 110 mm

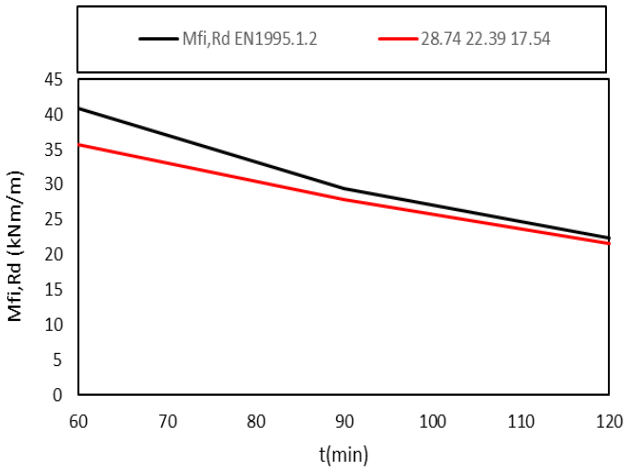

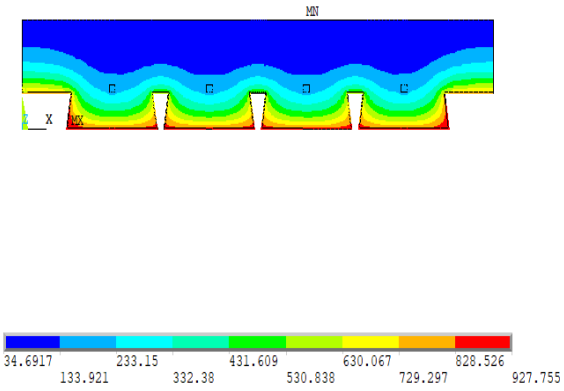

Slab22: h_1=110mm t=60 min

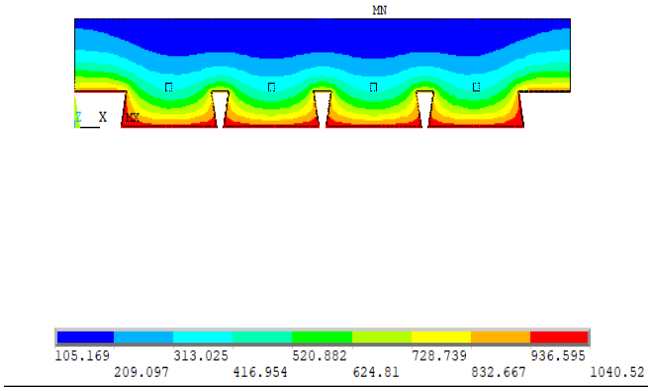

Slab24: h_1=110mm t=120 min

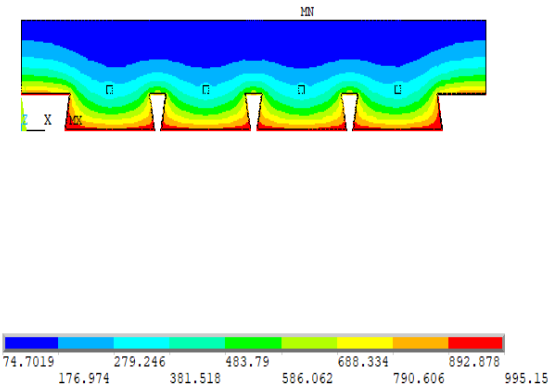

Slab23: h_1=110mm t=90 min

Steel deck: Reentrant – Multideck50

Finite element mesh- h_1= 50 mm

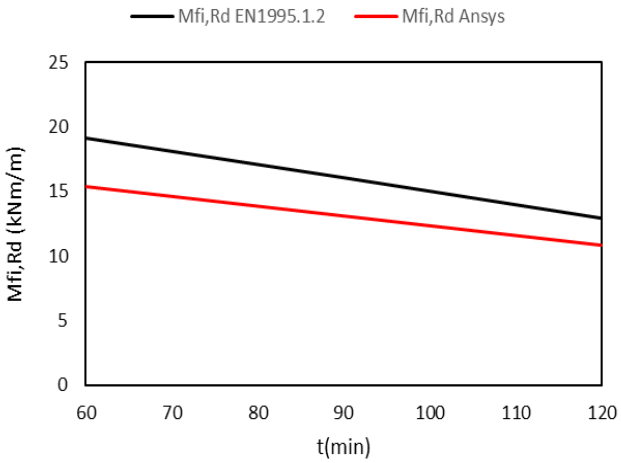

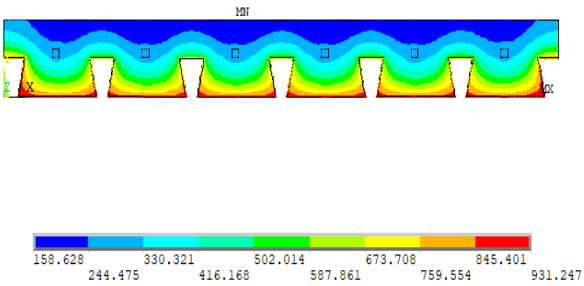

Slab25: h_1=50mm t=60 min

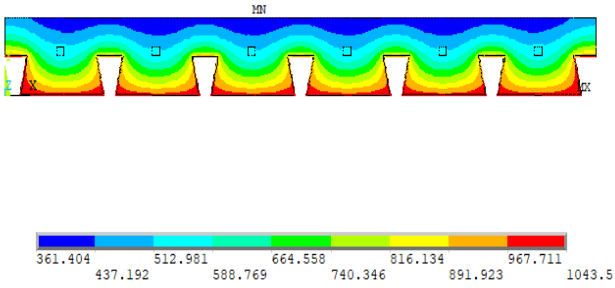

Slab27: h_1=50mm t=120 min

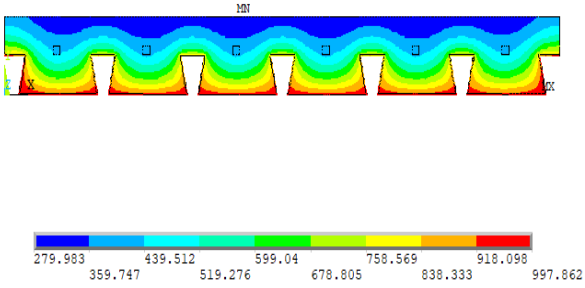

Slab26: h_1=50mm t=90 min

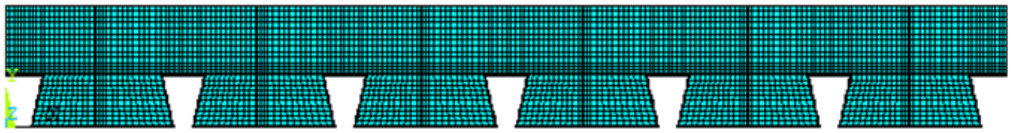

Finite element mesh- h_1= 70 mm

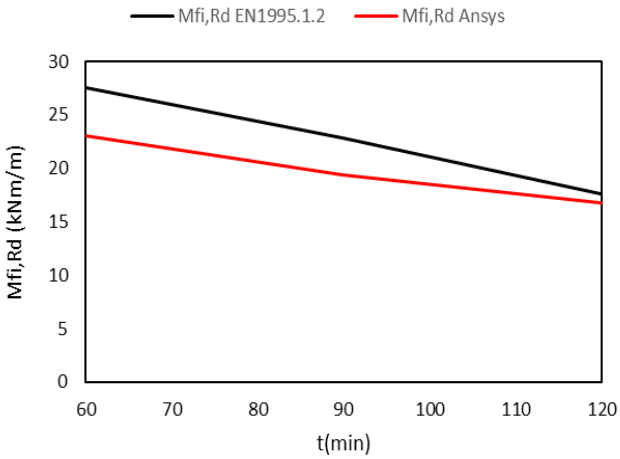

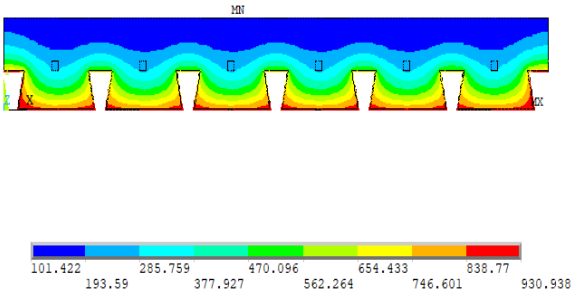

Slab28: h_1=70mm t=60 min

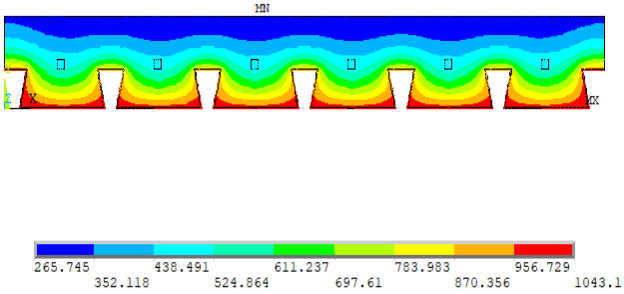

Slab30: h_1=70mm t=120 min

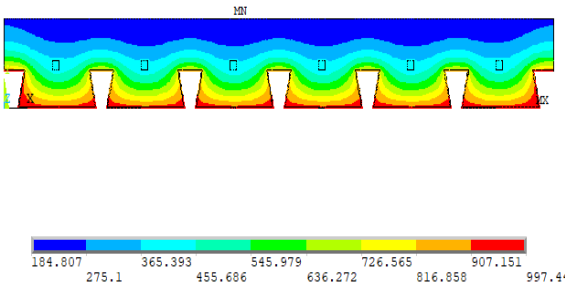

Slab29: h_1=70mm t=90 min

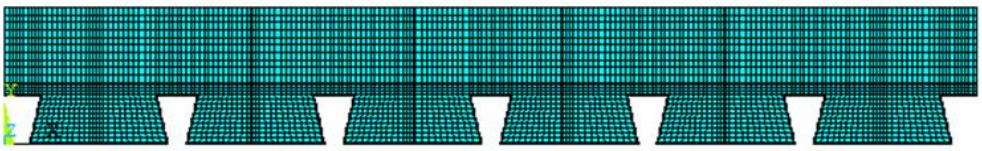

Finite element mesh- h_1=90 mm

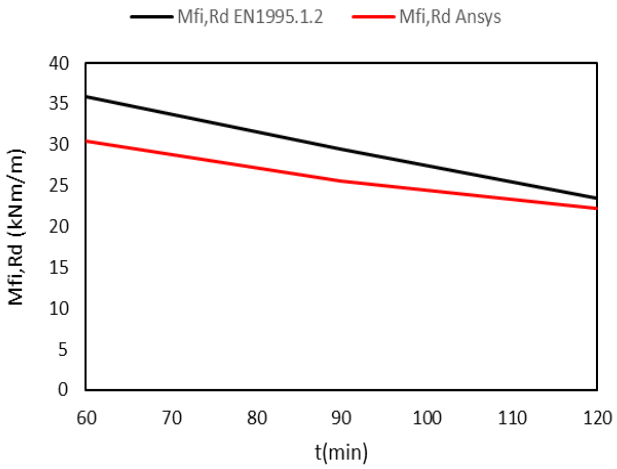

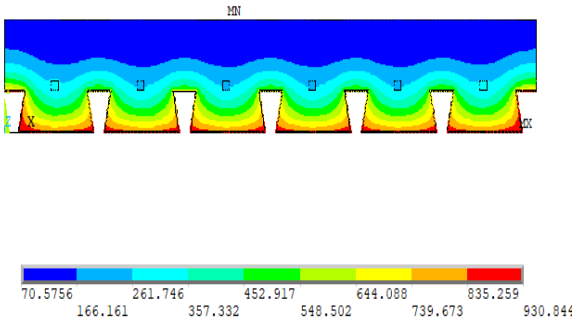

Slab31: h_1=90mm t=60 min

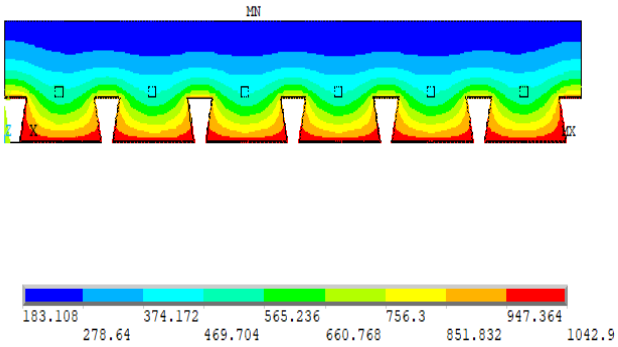

Slab33: h_1=90mm t=120 min

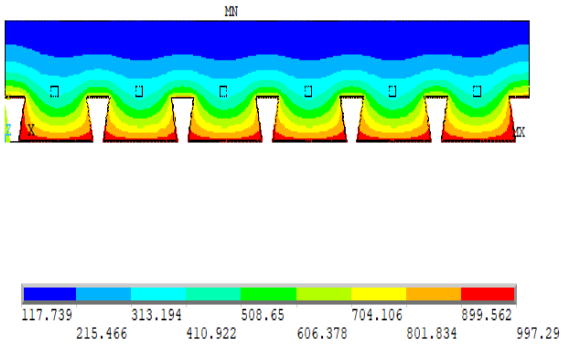

Slab32: h_1=90mm t=90 min

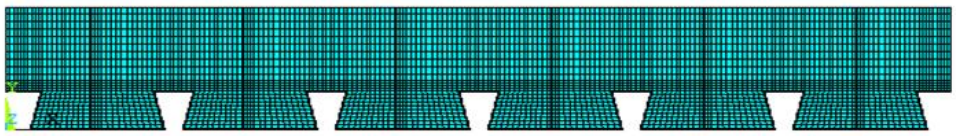

Finite element mesh- h_1=110 mm

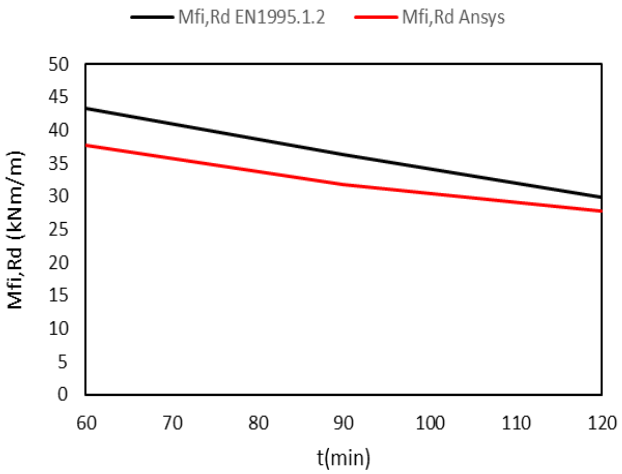

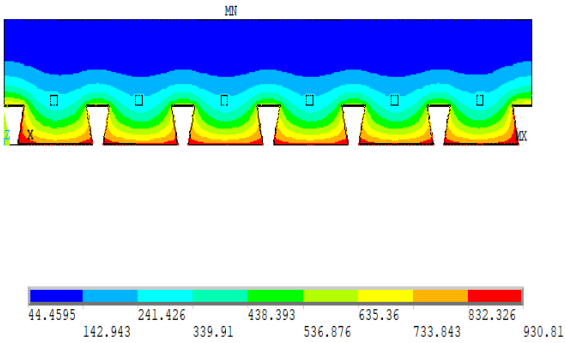

Slab34: h_1=110 mm t=60 min

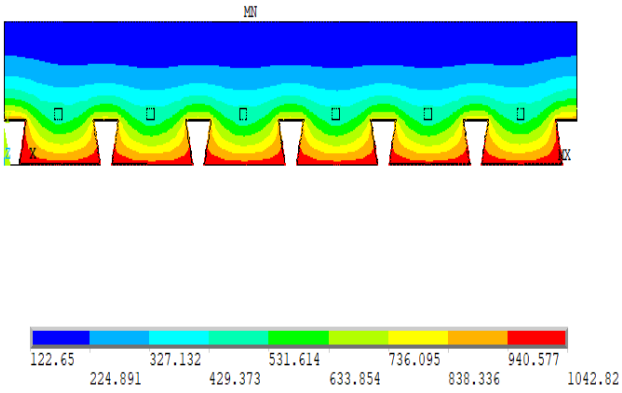

Slab36: h_1=110 mm t=120 min

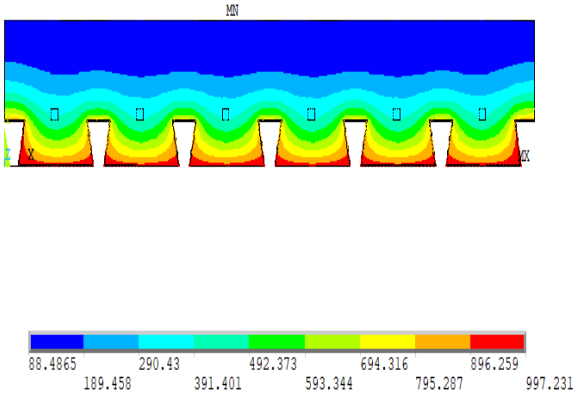

Slab35: h_1=110 mm t=90 min

Steel deck: Trapezoidal – Polydeck 59S

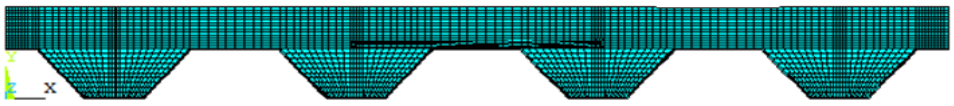

Finite element mesh- h_1=50 mm

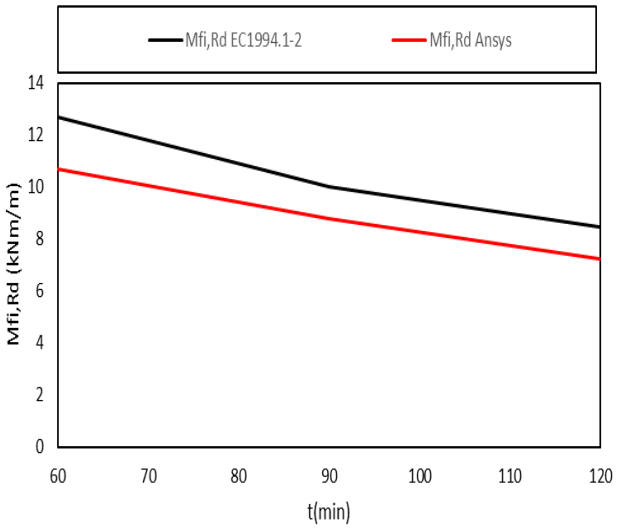

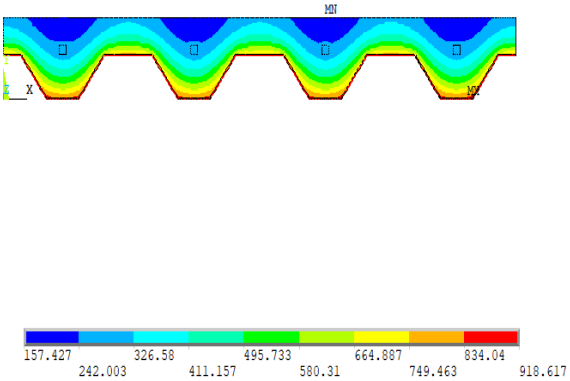

Slab37: h_1=50 mm t=60 min

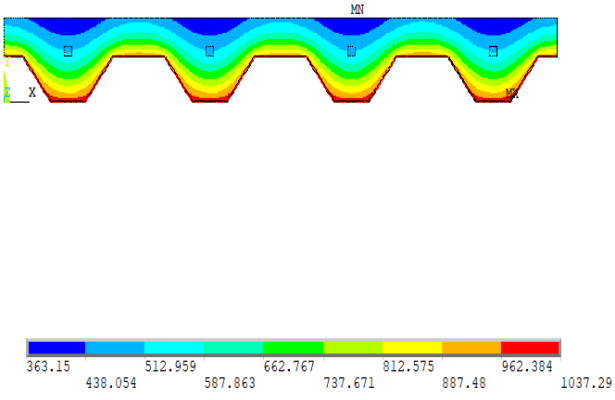

Slab39: h_1=50 mm t=120 min

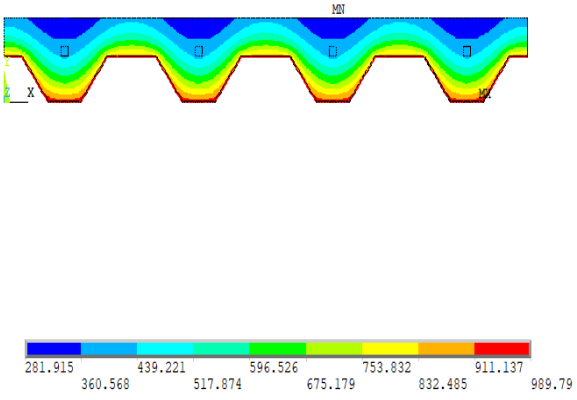

Slab38: h_1=50 mm t=90 min

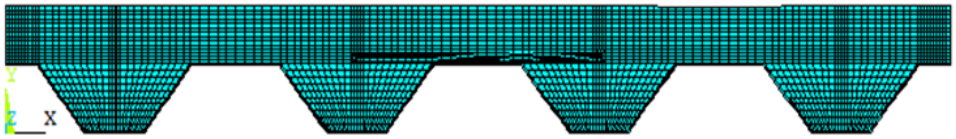

Finite element mesh- h_1=70 mm

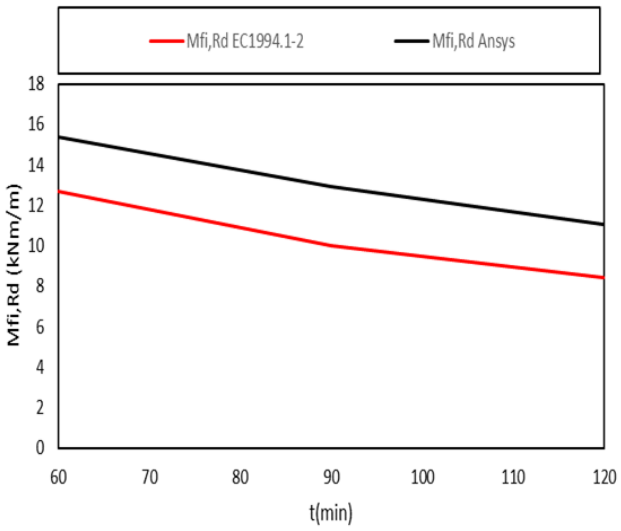

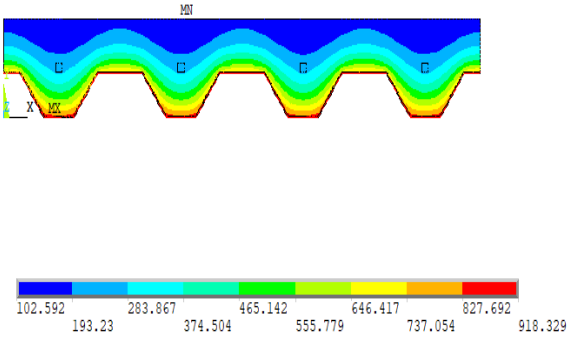

Slab40: h_1=70 mm t=60 min

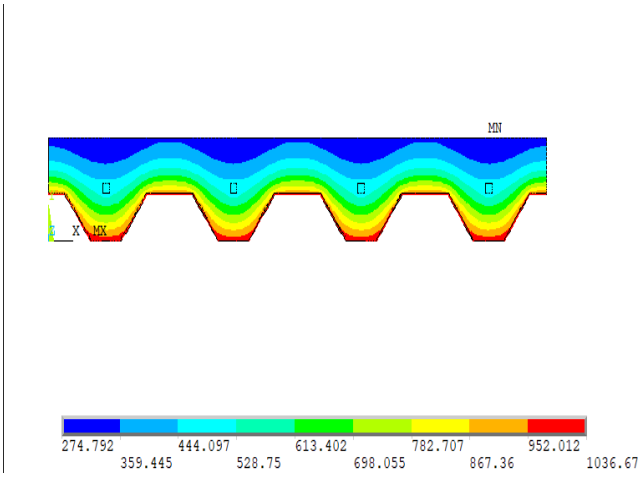

Slab42: h_1=70 mm t=120 min

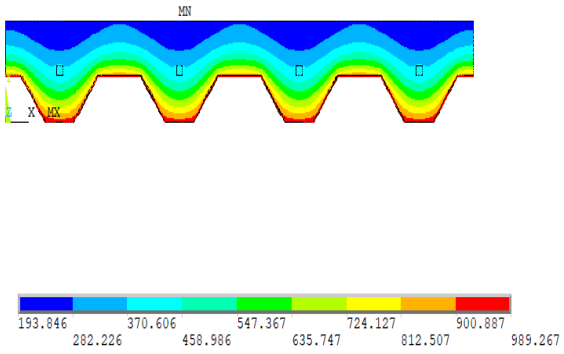

Slab41: h_1=70 mm t=90 min

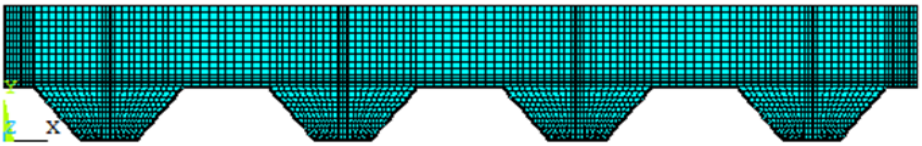

Finite element mesh- h_1=90 mm

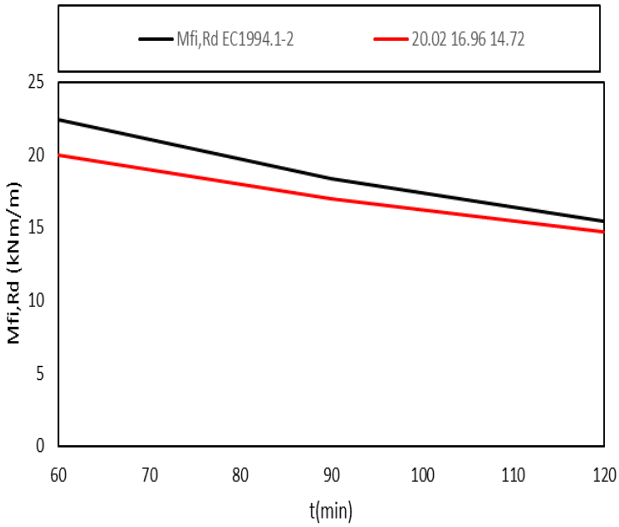

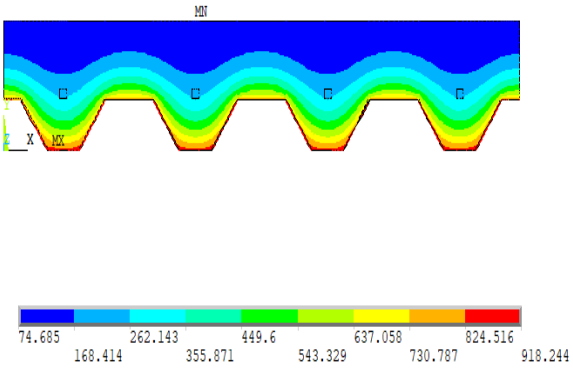

Slab43: h_1=90 mm t=60 min

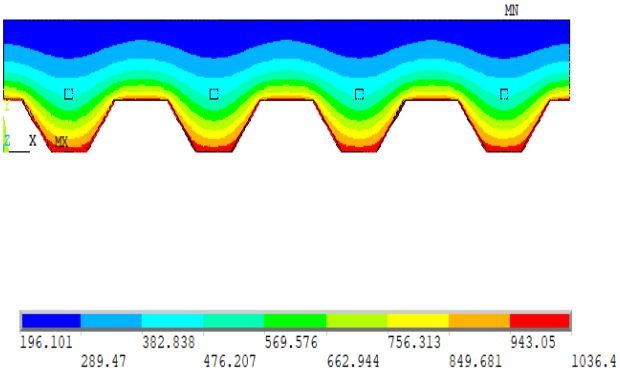

Slab45: h_1=90 mm t=120 min

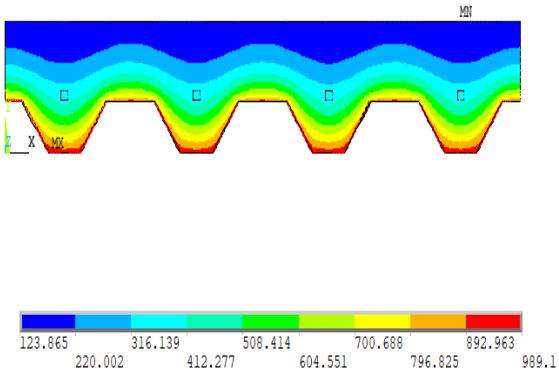

Slab44: h_1=90 mm t=90 min